MECHANISM AND KINETICS OF IRON DETERIORATION IN n-BUTANE AT ELEVATED TEMPERATURES

A THESIS

Presented to

The Faculty of the Division of Graduate

Studies and Research

By

Michael G. Gordow Klett

In Partial Fulfillment

of the Requirements for the Degree

Doctor of Philosophy in the School

of Chemical Engineering

Georgia Institute of Technology

June, 1973

MECHANISM AND KINETICS OF IRON DETERIORATION IN n-BUTANE

AT ELEVATED TEMPERATURES

Approved:

R. F. Hochman, Chairman

Helen Grenga

Charles W. Gorton

Date approved by Chairman: 7/6/73

ACKNOWLEDGMENTS

The author expresses his appreciation to his thesis advisor, Dr. R. F. Hochman, for his interest and helpful suggestions during this study. The comments and advice offered by Dr. Helen Grenga and Dr. C. W. Gorton who served as members of the thesis committee are also appreciated.

The author is grateful for the financial assistance provided by the National Science Foundation Graduate Traineeship Program during the academic years from 1969 to 1972. Thanks are also due Dr. G. L. Bridger for providing financial assistance during the last year of this work through a DuPont Chemical Company fellowship grant.

The author would also like to thank Mr. C. R. Blackwood and Mr. J. A. Nabors for help in building the experimental equipment and maintaining the mass spectrometer; and Mr. D. A. Rehbein for assistance in the metallographic work.

Most of all, the author wishes to thank his wife. Without her encouragement and help this work could never have been accomplished.

TABLE OF CONTENTS

LIST OF TABLES

LIST OF FIGURES

LIST OF FIGURES (Continued)

SUMMARY

The term "metal dusting" is used to describe the deterioration of iron, nickel, and cobalt in gases containing carbon at elevated temperatures. The basis of the term "metal dusting" is the resultant powder-like corrosion product, consisting of carbon and metal. The form of the attack on a metal surface includes localized or general pitting and/or general overall surface wastage. Failures have occurred most often in the petroleum and petrochemical industries especially in cracking and reforming units.

Research in the area of "metal dusting" generally has been limited to the simpler "metal dusting" environments of carbon monoxide, methane, and their mixtures with hydrogen. The reaction of carbon monoxide over iron has been studied extensively and the kinetics and mechanism of this reaction have been generally worked out. Although "metal dusting" failures from hydrocarbon attack have been reported in industry, methane and other light hydrocarbons have been shown experimentally to be relatively inert until well above normal "metal dusting" temperatures. The research reported here was conducted to determine if heavier hydrocarbons can cause experimental "metal dusting", and if so, to determine the kinetics and mechanism of the hydrocarbon attack so as to distinguish it from carbon monoxide "metal dusting".

The system selected for study was n-butane and pure iron wire. n-Butane decomposes at a much lower temperature than methane and thus would be more likely to "metal dust" at lower temperatures. Iron is the

most reactive of the dusting metals and much data on the iron wire reaction with carbon monoxide and methane are available for comparison.

Unlike carbon monoxide, n-butane will decompose homogeneously at "metal dusting" temperatures. A metal surface can not only react directly with the gas, forming carbides and catalyzing the formation of carbon, but also may alter the rate and products of the gas decomposition. Two different series of experiments were conducted to determine the extent of these two effects for the reaction of n-butane over iron.

The effect of iron wire on the pyrolysis of n-butane was determined by a low pressure pyrolysis technique. This technique permitted a steady state flow of reactant molecules to pass into a thermostated reaction cell under conditions of such low pressure that most collisions of reactant or product molecules take place with the vessel walls and not in the gas phase. The reactant and product molecules are pumped from the reactor into a mass spectrometer and analyzed. The pyrolysis was first carried out in a quartz reactor and then in the same reactor packed with various amounts of iron wire. It was found that bulk iron catalyzes the decomposition of n-butane by a surface reaction. The initial reaction products are mainly the C_2 hydrocarbons ethane, ethylene and acetylene.

To investigate the reaction on iron surfaces during the decomposition of n-butane a quartz tubular flow reactor packed with iron wire was used. The reactor was essentially at one atmosphere and heated by a tube furnace. Carbon formation and metal deterioration were measured gravimetrically. The wire was examined metallographically and the surface deterioration including the carbon deposits were examined in a scanning electron microscope. It was found that the reaction of iron

with n-butane above its decomposition temperature results in carbon formation on the iron surface. The carbon formation is accompanied by a general deterioration and pitting of the iron surface. Carbon formation does not occur without iron to act as a catalyst. The first signs of a reaction on the iron wire within twenty hours appeared at 595°C. The amount of carbon formed increases with temperature until 735°C. At higher temperatures the carbon formation drops off. The weight loss of the iron wire was affected by temperature in the same manner except that the maximum occurred at a lower temperature. At each temperature the weight of carbon formation is proportional to the loss of weight of the iron surface. The carbon formed consists of: (1) filamentary growth, and (2) flake or bulk deposits. The length and diameter of the filaments increase with increasing temperature. Above the eutectoid temperature surface deterioration stops and only a small amount of carbon is deposited.

The carbon formation appears to be mainly the result of polymerization and dehydrogenation of sorbed species. Metal loss occurs through the migration of iron from the surface into the filamentary carbon growth and by intergranular attack of the metal and grain removal by carbon deposits at the grain boundary. The temperature range of "metal dusting" attack is limited by the decomposition of n-butane at lower temperatures and the body centered cubic to face centered cubic phase change in iron at higher temperatures. Carburization of iron is the principal reaction when iron transforms to austenite.

n-Butane "metal dusting" on iron is much more severe than carbon monoxide attack. More than one hundred times as much carbon is formed during n-butane attack promoting more severe surface deterioration.

CHAPTER I

INTRODUCTION

The heavy deterioration of metals in gases containing carbon at elevated temperatures below normal carburizing temperatures has been termed "metal dusting". The resultant powder-like corrosion product, consisting of carbon (graphite) and metal, is the basis for the term "metal dusting". The gaseous phases are carburizing and can contain carbon monoxide, carbon dioxide, hydrocarbons, and often water and hydrogen. Iron, nickel, cobalt and most of their alloys are subject to this attack. The form that this attack takes includes localized or general pitting and/or general overall surface wastage. The temperature range for attack is usually from 450°C to around 800°C. Failures have occurred most often in the petroleum and petrochemical industries especially in cracking and reforming units. Similar forms of the attack have been found in the steel industry, in internal combustion engines, in waste heat boilers, and in certain nuclear reactors.

Research in the area of "metal dusting" generally has been aimed at defining the products formed, the reactivity, and the reaction kinetics for systems consisting of the common engineering alloys and the simpler "metal dusting" environments (gas phases of carbon monoxide, methane, and their mixtures with hydrogen). The reaction of carbon monoxide on iron under controlled conditions has been the most studied of the "metal dusting" forms of attack. Because of this, the kinetics and mechanism of carbon monoxide "metal dusting" has been generally worked out.

A second form of "metal dusting", hydrocarbon attack, has also been studied mostly using methane as an environment. Although the hydrocarbon methane had been considered as contributing to the reaction, this pure hydrocarbon gas had been shown experimentally to be relatively inert until well above the normal "metal dusting" temperatures.

The research reported here was begun to determine if heavier hydrocarbons can cause a "metal dusting" reaction, and if so, to determine the reaction kinetics and mechanism of metal deterioration for hydrocarbon "metal dusting" in order to distinguish it from carbon monoxide "metal dusting". There are sufficient indications that hydrocarbon "metal dusting" does occur and a logical system was selected to investigate the kinetics and mechanism of reaction.

The system selected to study was n-butane and pure iron wire. n-Butane was chosen since it decomposes at a much lower temperature than methane and thus would be more likely to cause "metal dusting" at a lower temperature, its homogeneous decomposition has been studied and is well-known, and "metal dusting" deterioration has been found in many butane industrial processes. Iron wire was chosen since iron is the most reactive of the dusting metals and much data on the iron wire reaction with carbon monoxide and methane are available for comparison.

The equilibrium composition of the system at the temperatures in question was calculated using a free energy minimization technique. A quartz tube flow reactor packed with coiled iron wire was used to determine if hydrocarbon "metal dusting" occurs and to measure the effect of the reaction on the wire. To determine the effect of the iron wire on the kinetics of the n-butane decomposition, a low pressure pyrolysis technique, with the effluent gas analyzed by mass spectrometry was used.

CHAPTER II

LITERATURE SURVEY

This thesis is concerned with the phenomena of hydrocarbon "metal dusting", specifically with the reaction of n-butane over iron. While a study of this system with regard to the "metal dusting" reaction is unique, obviously there are many areas in the literature that deal with subjects which concern this investigation. This chapter will survey the literature of those subjects which are pertinent to this investigation.

This first section will discuss the homogeneous decomposition of n-butane since an understanding of this reaction is necessary in discussing the reaction of n-butane with iron. The next section will present information on the iron-carbon system. Iron, carbon, and carbides are the solid phase reaction products of the reaction of n-butane with iron so this section will review information on these subjects. The third section discusses the reaction of hydrocarbons over iron and its alloys. The first four parts of this section deal directly with subjects that are included in the "metal dusting" reaction. Also presented in this section is a short discussion on gas carburization and the Fischer-Tropsch synthesis. While these two reactions of hydrocarbons over iron are important in industry, they do not contribute to the hydrocarbon "metal dusting" reaction. Gas carburization takes place at a temperature above the 450° to 800°C range of "metal dusting" and the Fischer-Tropsch synthesis takes place at a temperature much below this

range. The last section will review carbon monoxide "metal dusting" with a view to presenting the mechanism of the reaction as it is now believed to occur. An understanding of this reaction is necessary in order to distinguish it from hydrocarbon "metal dusting".

The Pyrolysis of n-Butane

Most of the work reported in the literature concerning the kinetics of the thermal decomposition of n-butane is largely restricted to the temperature and pressure ranges of 400°-600°C and 10-500mm Hg respectively. The conversion also has usually been kept low. These restrictions are due to inherent difficulties in the application of the static method to high temperature studies; and also to prevent the formation of higher hydrocarbons in secondary reactions in both static and flow methods. However, even with these limitations, the kinetics, mechanism and Arrhenius parameters of the n-butane pyrolysis have all been investigated and are now reasonably well known.

In early studies Pease (1) and Pease and Durgan (2) established that the n-butane pyrolysis is largely homogeneous and approximately of the first order. They found the overall reaction to be represented mainly by the stoichiometric equations:

$$C_4H_{10} = C_3H_6 + CH_4$$

$$C_4H_{10} = C_2H_4 + C_2H_6$$

Steacie and Puddington (3) found that the first pair of products produced about twice as fast as the second, so that the overall stoichiometry was approximately represented by the equation:

$$C_4H_{10} = 2/3\ CH_4 + 2/3\ C_3H_6 + 1/3\ C_2H_6 + 1/3\ C_2H_4.$$

Pacey and Purnell (4) found that while at lower temperatures the ratio of yields of ethane to ethylene were quite similar, that at 635°C selectivity to ethylene is much greater than that to ethane. Wittig (5) also found that in the 600°C-1200°C range there was a strong increase of the ethylene portion.

The first general mechanism to account for the presumed first-order kinetics of this and other organic pyrolysis reactions was proposed by Rice and Herzfeld (6). Subsequent work has strengthened their basic premises, which may be summarized as follows (7):

Initiation:

1. Free radicals are initiated by the splitting of the molecule at its weakest link.

Chain Propagation:

2. One of these radicals abstract H from the parent compound to form a small saturated molecule and a new free radical. Both radicals may so react.
3. Free radicals of the type $RCH_2 - CH_2$ can stabilize themselves by splitting off ethylene:

$$RCH_2 - CH_2 \cdot \longrightarrow R \cdot + CH_2 = CH_2$$

Termination:

4. Chain ending occurs through association or disproportionation of radicals.

A number of workers (7, 8, 9, 10, 11, 12) have proposed a Rice-Herzfeld free-radical chain mechanism for the n-butane pyrolysis, and

most of the schemes have many features in common. The following mechanism adequately accounts for the overall kinetics of the n-butane pyrolysis at around 500°C (4, 13).

Initiation

$$C_4H_{10} \rightarrow 2C_2H_5\cdot \quad (1)$$

$$C_4H_{10} \rightarrow CH_3\cdot + 1 - C_3H_7\cdot \quad (2)$$

Propagation

$$C_2H_5\cdot + C_4H_{10} \rightarrow C_2H_6 + C_4H_9\cdot \quad (3)$$

$$CH_3\cdot + C_4H_{10} \rightarrow CH_4 + C_4H_9\cdot \quad (4)$$

$$C_4H_9\cdot \rightarrow C_2H_4 + C_2H_5\cdot \quad (5a)$$

$$C_4H_9\cdot \rightarrow C_3H_6 + CH_3\cdot \quad (5b)$$

$$C_2H_5\cdot \rightarrow C_2H_4 + H\cdot \quad (6)$$

$$H\cdot + C_4H_{10} \rightarrow H_2 + C_4H_9\cdot \quad (7)$$

Termination

$$C_2H_5\cdot + C_2H_5\cdot \rightarrow C_4H_{10} \quad (8a)$$

$$C_2H_5\cdot + C_2H_5\cdot \rightarrow C_2H_6 + C_2H_4 \quad (8b)$$

Hydrogen is a significantly less important product than ethane (11); reaction 3 therefore occurs more rapidly than 6. Thermodynamics indicate that reaction 2 should be about a factor of 10 slower than reaction 1 (14).

This scheme for the decomposition of n-butane cannot be solved explicitly for the overall reaction rates. The order of the reaction with respect to n-butane may appear to be anything from 1/2 to 3/2 (7). The order of the n-butane pyrolysis has been reported as one (1, 2, 3, 5) and 3/2 (10, 11, 12, 15). For normal temperatures and pressures the order of the reaction is now considered to be 3/2.

Activation energies have been reported ranging from 45.6 to 59.9 Kcal/mole (3, 11, 12, 16, 17). A generally accepted value of 58.7 Kcal/mole was obtained by Steacie and Puddington (3) using a static method. In flow systems figures as low as 45.6 Kcal/mole were obtained (17). After considering the heat-transfer aspects of externally heated tubular reactors used for hydrocarbon pyrolysis, Calderbank (18) suggested that measurements of reaction rates under such conditions are in reality, measurements of the rates of heat transfer. This is due to the existence across the reactors of large temperature differentials resulting from the endothermic nature of the reactions. It follows that there should be a difference in the values of the activation energy as determined by static and flow methods. Unfortunately, inherent difficulties in the application of the static method to high temperature studies do not permit a ready comparison of these two methods.

In a study of n-butane pyrolysis at 527°C and 10-30 mm Hg reactant pressure, Purnell and Quinn (19) found that the distribution and rates of formation of products were identical in Pyrex vessels with surface to volume ratio (s/v) varying from 1.2 to 4.4 cm^{-1}. Sandler and Chung (16) found no catalytic effect of the surface of a packed Vycor tube with a s/v of 32.6 cm^{-1} as compared to an unpacked tube with s/v of 19.9 cm^{-1}.

However, Sagert and Laidler (12) using quartz vessels with a 11.6-fold increase in s/v, found a small but significant change. At all temperatures between 520 and 590°C they found that the rate of decomposition was lower in the packed vessel. The fall in rate was greatest at low temperatures corresponding to an activation energy in the packed vessel of 62.3 Kcal. $mole^{-1}$ as compared to 59.9 Kcal. $mole^{-1}$ in the unpacked vessel.

Sagert and Laidler also showed that conditioning of the unpacked reaction vessel surface by extended pyrolysis of n-butane led to rates which were greater at higher temperatures and less at lower temperatures than those observed with the unconditioned vessel. They concluded that these results confirm the conclusion that some of the initiation and termination is taking place at the vessel walls. Purnell and Quinn (19) also found that conditioning by prolonged pyrolysis of n-butane led to a significant fall in the rate of subsequent n-butane pyrolysis and that the effect of successive conditioning was cumulative. Conditioning of the reaction vessel resulted in the deposition of a thin layer of carbon on the walls. The reaction rate would fall until the vessel was completely covered with a fine layer of carbon, whereafter further deposition would not affect the rate of the reaction. It is generally felt that, with reaction vessel surfaces that are stable and not coated with carbonaceous material, the pyrolysis of n-butane is essentially homogeneous at normal temperatures and pressures. Of course, if s/v were increased sufficiently, then some heterogeneous contribution to the overall rate would probably be introduced even in these systems (20).

Several workers have reported on carbon and higher hydrocarbons

being formed at higher temperatures and conversions. King et al. (21) reported that, during a n-butane pyrolysis in a flow reactor at 809°C, the carbon to hydrogen ratio obtained by analysis of the gaseous effluent diminished gradually with an increase of conversion, indicating that condensible polymers of high carbon content were being formed in increasing amounts. These appeared as a fog in the effluent gas stream. Sandler and Chung (16) found small quantities of higher boiling products in a vycor flow reactor at 700°C. Wittig (5) also found components with a higher carbon portion at higher temperatures and longer reaction times with a shock tube pyrolysis of n-butane.

The Iron Carbon System

Iron-Carbon Equilibrium Diagram

The iron-carbon system may be characterized by either the iron-graphite or the iron-iron carbide equilibrium diagram. The major features of the iron-iron carbide phase diagram, Figure 1, have been well established (22, 23, 24, 25). The "equilibrium" phase, cementite (Fe_3C), on the right end of the diagram, is in reality metastable and decomposes to iron and graphite under certain conditions (26, 27). At temperatures below the eutectoid, the iron is a body-centered cubic phase known as ferrite (α). Above the eutectoid transformation temperature of 723°C, the face-centered cubic iron structure, austenite (γ) can be formed. Both phases dissolve carbon interstitially. Between 723°C and 910°C and at appropriate carbon concentrations, a two phase mixture of austenite and ferrite exists. The maximum dissolved carbon in ferrite is 0.025 weight percent at 723°C while at 50°C the solubility is 10^{-4} weight percent (28). Austenite has a capacity for 0.8 to 2.0 weight percent carbon depending

on the temperature.

Cementite, although less stable than graphite, is formed in preference to graphite in a pure system because of kinetic factors. The presence of impurities in the iron, for example silicon, will promote graphite formation (27, 29). With slight modifications, the iron-graphite equilibrium diagram is the same as the iron-cementite system exhibited in Figure 1. Figure 2 compares the equilibrium factors of cementite and graphite in a pure system for the region of interest. Note the near coincidence of the graphite and cementite solubility lines.

The phases and compounds observed at room temperature are not necessarily those which existed at experimental conditions, and identification of the high temperature phases must be established through its relation to the room temperature phases.

Carbides of Iron

Cementite (Fe_3C), the most stable of the iron carbides, was the first carbide structurally defined (34). The general physical and chemical characteristics are well established for Fe_3C (35, 36). The most widely used method for producing Fe_3C is by the reaction of ferrite with carbon-containing gases at appropriate temperatures.

The next carbide discovered was the Hagg carbide in 1934 (37). It has been known as percarbide and as $Fe_{20}C_9$. Jack and Wild (38) recently established this carbide to be Fe_5C_2. Hagg carbide is produced by treating high-purity iron or iron oxide with a mixture of CO and H_2. At ratios of $CO:H_2 = 1:4$, only the Hagg carbide is formed in the temperature range of 300°-360°C (39). Hagg carbide changes into Fe_3C above 360°C (40).

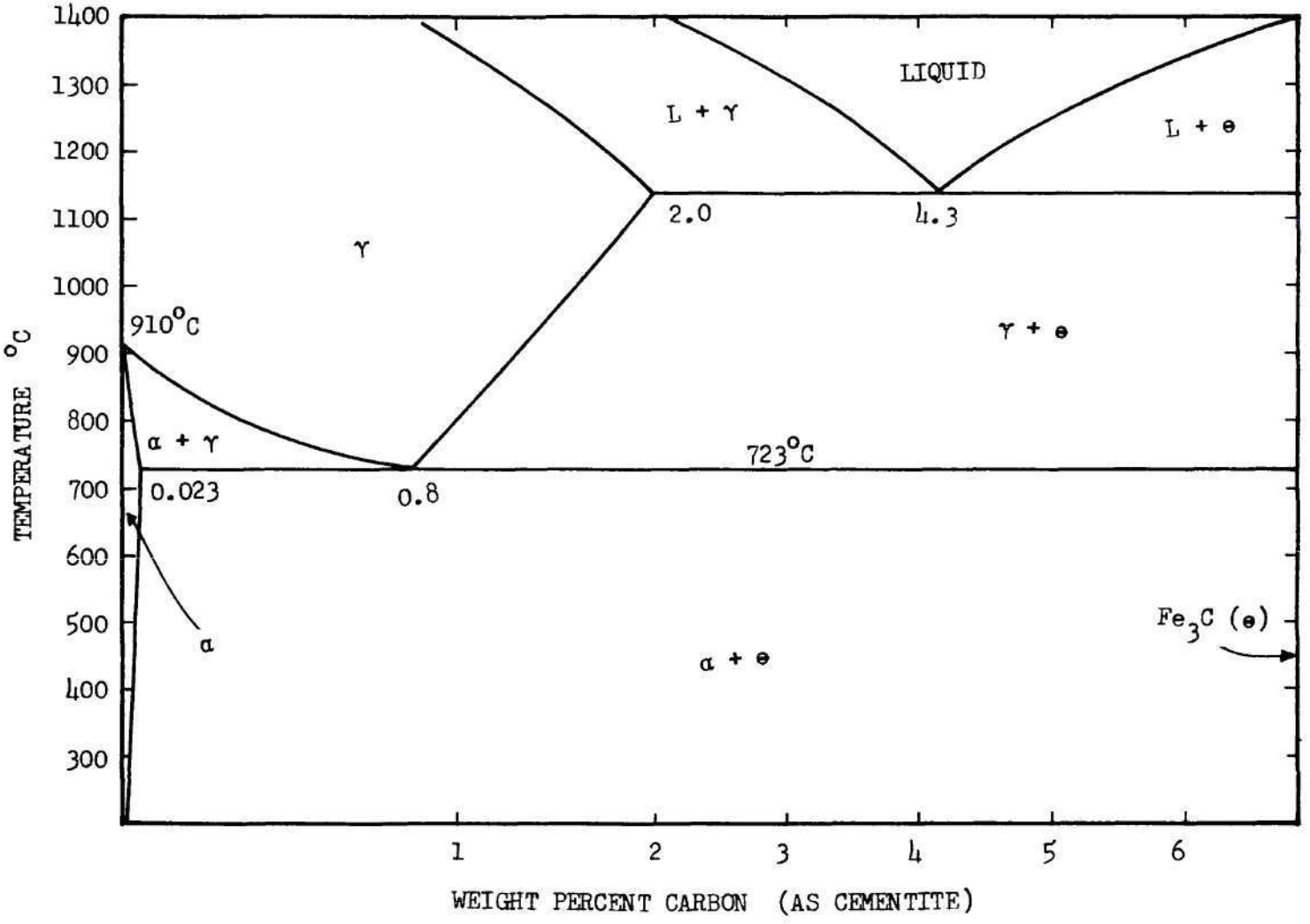

Figure 1. Iron-Cementite Equilibrium Phase Diagram

▽ - (30) ○ - (32)

□ - (30) ◇ - (22)

△ - (31) ● - (32)

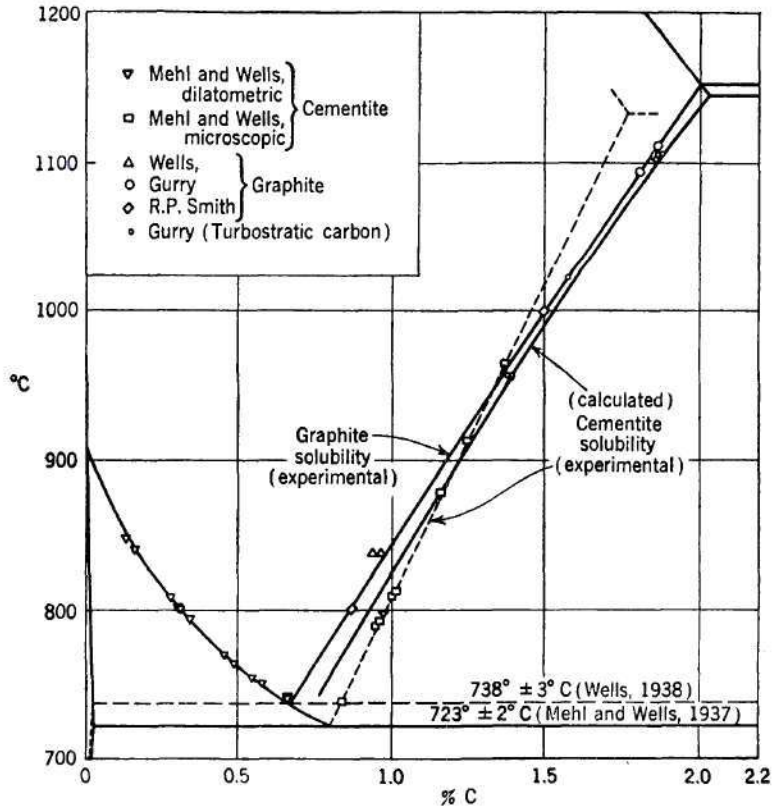

Figure 2. Cementite and Graphite Solubility in Gamma-Iron (33)

Epsilon-carbide was first characterized in the literature by Hofer and associates (36, 41, 42). Its structure has been established as hexagonal close-packed and its composition is thought to be Fe_2C (43). It has been observed as a result of low temperature carburization of finely divided iron. At 300°-400°C Epsilon-carbide is transformed in Hagg carbide, which in turn changes into cementite (44, 45).

Echstrom and Adcock (46) found a carbide in the catalyst of a fluidized-bed, hydrocarbon synthesis plant. The substance has been characterized as Fe_7C_3 (47). Attempts to synthesize this material in the laboratory have failed thus far.

The Reaction of Hydrocarbons Over Iron and Its Alloys

Surface Effects on the Thermal Decomposition of Hydrocarbons

Tamai and Nishiyama (48) studied the role of the surface of the reaction vessels in the thermal decomposition of hydrocarbons. The decomposition of propane was conducted in a flow system, using three kinds of reaction vessels; iron, gold and silica. The temperature range studied was from 580° to 730°C. The effects of packing were also examined. The product distributions at the initial stage were nearly the same among the different reaction vessels, but the rate of decomposition differed remarkably. The rates in the iron reactor were larger than those in silica. In the case of the gold vessel, the decomposition was relatively slow, and much slower with the packed vessel. A tentative explanation for the difference in rate between the gold and iron reaction vessels is that iron can initiate and terminate the radical chain reactions but gold can only terminate them.

As the conversion increased, the composition of the gas phase

varied among different reaction vessels, perhaps because of different catalytic activity of the walls for secondary reactions. For the cases in which carbon formation was very slow, a quasi-equilibrium composition was calculated by assuming that equilibrium was obtained only among gaseous hydrocarbons. The results roughly agreed with the experimental compositions at the later stage of the decomposition of methane and ethane in gold vessels, which were conducted in a static system. The methane decomposition in a steel vessel seemed to proceed toward a composition in which gaseous hydrocarbons and graphite were in equilibrium with each other.

Crynes and Albright (49) investigated surface effects during the pyrolysis of propane in tubular flow reactors constructed of stainless steel and low-carbon steel at reaction temperatures from 600° to 750°C. At low conversions in the stainless steel reactor essentially equal amounts of methane, ethylene, hydrogen, and propylene were formed. At 750°C and at high conversions, butadiene and butane were found in trace quantities. Small amounts of carbon and liquid products were also formed. Runs made in low-carbon steel reactors indicated an appreciably higher wall activity than had been observed in 304 stainless steel reactors. Large amounts of carbon were formed in these reactors. The low-carbon steel reactor walls were very effective in promoting secondary reactions, especially of propylene and ethylene which form carbon, hydrogen and methane. This conclusion was based on the low olefin concentrations and high carbon and hydrogen formation which occurred during experimental runs in low-carbon steel reactors.

Nishiyama (50) studied the thermal decomposition of ethane in a

static system at 700°C, using a silica vessel packed with a sheet of iron. The gaseous products were composed of nearly equal moles of ethylene and hydrogen, a small amount of methane, and unreacted ethane. The iron packing decreased the rate markedly. It was concluded that the iron surface exerted a stronger influence on termination of the radical chain mechanism than in initiation, resulting in a reduction of the overall rate over the entire pressure range.

Carbon Deposition on Iron Surfaces from Hydrocarbons

It has been known for some time that certain transition metals including iron are able to influence cracking reactions; thus it is no surprise that they can affect carbon deposition. Most investigators concerned with the formation of carbon from gaseous hydrocarbons agree that the original molecules first decompose (51). Grisdale (52), while studying the production of pyrolytic carbon films, found that while the deposition of pyrolytic carbon films is not a surface reaction in the usual sense, the nature of the substrate surface can profoundly affect the reaction through its catalytic influence. For a ceramic surface contaminated with iron or other heavy metals or their oxides this influence is evidenced by the production of soft, sooty, easily removed deposits which can be formed at temperatures considerably below those normally required. There is evidence that these loosely adherent films may result through the formation of metal carbides as intermediates. Contaminant coke is a major factor in catalytic cracking operations (53). Contaminant coke refers to that produced as a result of metal poisons that are present on the catalyst and it usually amounts to about 30 percent of the coke formed during catalytic cracking. Iron constitutes the major contaminant in catalytic operations.

Tamai and his co-workers (54,55) studied the formation of carbon on iron and nickel surfaces from methane, ethane and ethylene for temperatures ranging from 870° to 1030°C. The rate of deposition was measured by the weight increase of the metal sheet. For iron the deposition rate depended on both pressure and temperature remarkedly for methane and ethane. The deposition rate for ethylene was nearly independent of temperature and pressure. There was some indication that metal atoms are carried into the carbon layer and continue to catalyze the deposition to some extent. X-ray results seem to favor a mechanism in which metal carbide is the intermediate of carbon formation. Hydrogen accelerates the reaction where the initial rates of deposition are pressure-dependent, but its effect becomes small under the conditions that the amount of deposition is large.

Robertson (56) studied the structure of carbon deposited on iron surfaces by thermally decomposing methane over iron at temperatures from 650° to 750°C. Transmission electron microscopy established the presence of two distinct types of carbon deposit-termed as "flake" and polycrystalline. Electron and x-ray diffraction properties of the "flake" carbon show a crystalline graphite-like structure. Surface perfection and reactivity studies also revealed the equivalence of "flake" carbon to natural or synthetic graphite. Usually crystalline graphite begins to appear only at decomposition temperatures of 2000° to 2500°C. There was also evidence of the iron substrate within specimens of the "flake" deposit. "Polycrystalline" carbons were characterized by their electron diffraction properties, which were indicative of a non-graphitic structure. The "polycrystalline" carbon showed fibers growing from the main body of the

deposit similar to those reported from carbon monoxide breakdown over iron. Electron microprobe analysis showed evidence of the metal substrate within the fibers.

The Reaction of n-Butane Over Iron and Its Alloys

King, et al. (57) studied the thermal decomposition of n-butane in a continuous flow system using reactors constructed of Vycor, stainless steel, and chromium-iron. The experiments involved temperatures in the range of 650°-850°C. The apparent energy of activation for the reaction was of the order of 40.0 Kcal/mole and the frequency factor was about 10^9. It was suggested that these low values are characteristic of decompositions carried out in continuous flow reactors under these conditions. The results also showed that these low values cannot be attributed to the effect of the surface but may be related to the problem of heat transfer.

The 18-8 stainless steel reactor at high conversion conditions was found to exert a deleterious effect on the desired reaction. The reactions leading to the end products carbon, methane, and hydrogen were promoted at the expense of those responsible for the production of the intermediate decomposition products, including the olefins. Under suitable conditions, results comparable to those obtained in the Vycor reactor could be obtained, but the rapid accumulation of hard carbon deposits on the hot reactor surfaces tended to block the reactor and necessitated its frequent dismantling for cleaning.

At high conversions it became very difficult to carry out the reaction in the stainless-steel reactor because, even in the relatively short time required to sample the effluent, the reactor became choked

with carbon. The extremely low values of the ratios of ethylene to methane plus hydrogen, and carbon to hydrogen, in the gaseous effluent afforded ample evidence of the high rate of formation of undesirable secondary reaction products, including carbon.

It was considered at first that the nickel in the steel was solely responsible for this effect. Consequently, a reactor was constructed of 12-14 percent chromium-iron alloy containing no nickel. In the chromium-iron reactor the results were quite satisfactory during the first hour or so of operation. However, the same difficulties with respect to carbon deposition and lowered olefin production were encountered with continued use. Continuous operation at high conversions could not be maintained in stainless steel or chromium iron reactors.

A stainless steel reactor was plated with three thousandths of an inch of chromium to eliminate completely the steel surfaces which came into contact with the hot gases. In a normal stainless steel reactor, operation at 50 percent conversion for any prolonged period was not possible due to excessive carbon formation. In the chromium plated reactor there was a substantial improvement in ethylene selectivity and ethylene to methane plus hydrogen ratio. The decompositions were carried out at conversions of over 90 percent for periods of intermittent operation exceeding several weeks, without difficulty.

It was concluded that while the initial decomposition reaction is essentially homogeneous, as the fraction of the feed converted is increased, the reaction mechanism appears to be altered depending upon the nature of the heated surface with which the reactants and products come into contact. While Vycor, a mainly silica surface, exerted a negligible

effect in the decomposition of n-butane, the steel surfaces exerted a marked catalytic effect on the reactions leading to carbon formation. Evidence showed that chromium was the only major constituent in this steel which did not give this effect.

Kukina et al. (58) studied the catalytic transformation of butane over α -iron. He found that up to 400°C n-butane decomposed on an α -iron catalyst to form hydrogen, traces of C_1, C_2 and C_3 hydrocarbons and carbon which enters the crystal lattice forming Fe_2C. The extent of the carburization of the catalyst was verified. Above 500°C the dehydrogenation of n-butane on α-iron was complicated by the formation of saturated hydrocarbons and carbon on the catalyst.

Hydrocarbon "Metal Dusting"

Numerous "metal dusting"failures, have been reported in hydrocarbon environments. Camp, Phillips and Gross (59) reported one of the first cases of catastrophic "metal dusting" corrosion. Stainless steel furnace tubes in a superheater for reforming naphtha in the production of butadiene, operating at approximately 700°C, were the subject of severe metal wastage, both by uniform thinning of the pipe cross-section and by pitting.

Another report by Burns (60) related heavy corrosion to sulfur in crude charges. The carbon steel equipment operated for less than a year with several major shutdowns due to severe pitting. Although the operating temperature was only 300°C, "hot spots" of 750°C were probable. Major blame is placed on the iron sulfide found, but mention is made of sooty carbon deposits in and around the corroded area and it is believed that this is a case of "metal dusting".

Hoyt and Caughey (61) cited a case of deterioration of 310 stainless steel in a process producing gasoline from coal. The attack was first observed after 125 days at temperatures of 650° to 700°C. Intergranular attack, as well as severe pitting and general metal loss were found. Attack was inconsistent in the same tube. He concluded that optimum conditions vary from gas to gas and theorized that the metal is corroded away by threads of carbon which are attached to metal particles and are easily lifted from the surface and carried away.

Prange (62), Eberle and Wylie (63), and Schley and Bennett (64) discussed a number of severe corrosion experiences in 300 and 400 series stainless steels subjected to hydrocarbon atmospheres in the temperature range of 450° to 700°C.

A survey was conducted by the American Petroleum Institute's Subcommittee on Refinery Corrosion (65) for cases of high temperature carburization failures. Replies were received from fifteen companies of which nine reported no failures and six reported failures in twelve units. The processes for which failures were reported were cracking, catalytic reforming, and dehydrogenation. The temperatures ranged from 500° to 1000°C and pressure from atmospheric to 500 psi. Most of the materials which failed were austenitic stainless steels.

Hochman (66, 67) reported on the reaction of some light hydrocarbons with coiled iron wire in a tubular flow reactor. With methane he found little, if any, reactivity in the 500° to 750°C range even in long term exposure. Ethane and propane also showed little or no reactivity at these temperatures. Above 750°C, carburization of the iron occurred. In addition, reaction products formed at these temperatures in methane

include higher hydrocarbons such as napthalene and anthracene. Observing these materials and their reaction with the iron surface reveals a rough and wavy deposit which has the appearance of a washing or erosion effect. Hochman concluded that the reaction in pure methane does not begin until decomposition of the methane occurs which was above 750°C. At these temperatures the reaction was more one of "gas carburization" instead of "metal dusting" and indications of "metal dusting" in these environments must be considered a result of H_2O, O_2, CO, and CO_2 in the system.

Thron (68) studied the reaction of methane and a 5 percent hydrogen-methane mixture in a tubular flow reactor packed with coiled iron wire. He found that significant reactivity of iron in methane occurs only at temperatures above 650°C, the minimum temperature for initiation of the thermal decomposition of methane. A 5 percent H_2-CH_4 mixture did not significantly affect the carbon formation of the reaction; however, hydrogen was found to promote surface attack on iron in methane atmospheres. The surface deposits were spherical and of roughly the same size. It was concluded that the reaction of methane with iron is a combination of surface carbon-hydrocarbon deposition, internal carburization, and carbide formation.

Two typical forms of "metal dusting" in a carbonaceous gas stream have been established (69). One is pit formation and heavy intergranular attack of the metal accompanied by carbon filament extraction of the metal or intergranular removal of grains. This occurs on either rough surfaces or when flow rates are relatively low. The second variation of the reaction is uniform thinning of the metal with little or no carburization of the surface, and only slight intergranular attack. This type of attack is

usually associated with a highly dynamic flow system which results in the combined effect of dusting and erosion.

Gas Carburization

The carburization of iron and steel may be effected by heating in a gaseous carbon-containing medium, which at high temperatures provides a supply of nascent carbon for absorption by the material being carburized. By controlling the temperature and time of treatment, the concentration of carbon in the surface of the steel and the depth of penetration may be varied over wide limits. Gases most commonly used are natural gas, "manufactured gas", and certain propanes. Butane is used infrequently but when used it should be n-butane, not isobutane. The temperature most common for carburizing is 925°C, which is in the austenite region of iron. An excessive amount of free carbon (in the form of soot or coke) deposited on the work has always been a problem in gas carburizing. The degree of sooting is determined by the concentration of the hydrocarbon in the carburizing atmosphere and this may be reduced by dilution with a suitable carrier gas (70).

Jenkins (71) studied the carburization of low carbon steel by n-butane. Experiments with pure n-butane resulted in a rapid sooting-up of the reaction tube. He found that it was not possible to reduce the concentration of n-butane sufficiently to eliminate sooting, without also suppressing completely the carburizing reaction. Much of the soot deposit was loose and could be readily brushed off the specimen, leaving the surface covered with a thin adherent coating of carbon.

Jenkins also studied carburization of steel below the austenitic change point. He found that in the ferrite-austenite region, the rate of

solution of carbon by iron is comparatively slow. Between 875°C, the upper critical point for the steel in question, and the lower transformation point of 723°C, the steel consists of ferrite and austenite, the latter increasing in concentration up to 100 percent at 875°C. At any temperature within this range the ferrite is saturated with carbon, while the austenite is of fixed carbon content and a state of equilibrium is set up between the ferrite and austenitic phases. Absorption of the carbon at the surface can take place only via the austenitic phase, which thereby becomes super-saturated with carbon with respect to the adjoining ferritic areas. The excess carbon diffuses to the austenite-ferrite boundaries, where transformation takes place progressively with the conversion of ferrite to austenite. This rather complex mechanism probably accounts in some measure for the low rate of carburization in the austenite-ferrite range as compared with that in austenitic structure (71).

Fischer-Tropsch Synthesis

The synthesis of high molecular weight paraffins and alcohols, accomplished by passing a mixture of carbon monoxide and hydrogen over a metal catalyst was first discovered at the Badeiche Anilin and Soda-Fabrik (72) in 1913 and now has achieved industrial prominence. Metals which are active in the Fischer-Tropsch reaction include iron, cobalt, nickel and ruthenium. Iron, which yields olefins and alcohols, is usually promoted by means of the addition of one of the irreducible metal oxides which act as structural promoters enhancing the stability of the metal phase. In addition, an electronic promoter is added, usually an alkali metal such as sodium or potassium, which effects an alteration in the electronic energy levels of the metal catalyst. Iron catalysts for the

Fischer-Tropsch synthesis do not usually require supports (73). Optimum temperature range for the synthesis is 200°-325°C for iron. Iron catalysts prepared by fusion of magnetite have been found active at pressures in the range, 20 to 100 atmospheres, whereas the activity of iron catalysts prepared by precipitation from solutions decreases with pressures above 20 atmospheres (74).

The carbon number and isomer distribution in the products of the synthesis can be calculated with fair accuracy from certain assumptions as to the mechanism of growth of the carbon chains. These assumptions are (75):

1. Stepwise addition of one carbon atom occurs at the terminal or next to terminal carbon atom of a molecule adsorbed on the surface of the catalyst.
2. The rates of addition at terminal or next-to-terminal carbon atoms are independent of the length of the carbon chain and of the degree of branching, except that addition at a next-to-terminal carbon atom already attached to three carbon atoms occurs only very slowly compared with the rate of addition to other than tertiary carbon atoms.

With these assumptions the probability of chain growth can be shown to decrease logarithmically with increasing carbon number and this is precisely what is found in practice. This theory predicts the isomer and carbon number distribution for iron only up to 10 carbon atoms. For higher carbon numbers the equation calls for lower mole fractions than are obtained experimentally.

Carbon Monoxide Metal Dusting Over Iron

Carbon monoxide disproportionation is thermodynamically feasible below 1000°C at one atmosphere pressure. However, the reaction proceeds at a measurable rate between 450°C and 800°C only in the presence of a catalyst. Iron, nickel, and cobalt are the most active catalysts; whereas chromium, molybdenum, tungsten, zinc and silver are only slightly active (76). The study of the carbon monoxide reaction over iron can be divided into two main categories; studies of the overall kinetics of the reaction and studies of the early stages of reaction including the mechanism of catalysis.

The kinetic studies have measured rates either by the consumption of carbon monoxide (77, 78) or by the weight gain including all carbonaceous surface products of the metal used as a catalyst (66, 68, 76, 79). Although this does not determine the deterioration of the metal directly, the decomposition of the gaseous phase with carbon formation on the metal appears to be proportional to metal deterioration. The rate of the reaction with pure bulk iron varies with time, being slow initially, increasing to a maximum and then decreasing to a steady state value. The rate increases with temperature from 400°C to a maximum at 550°C and then decreases. Westerman (79) found a minimum at 710°C and then a gradual increase in the reaction again above 710°C, but now with heavier carburization as one might expect. Haas (77) found that Arrhenius plots for the reaction showed that the activation energy increased in the temperature range of 400°C to 550°C as the amount of carbon deposition increased. Westerman (79) also indicated increasing activation energy with increasing carbon deposition in this temperature range. Haas (77) has also found

a pressure dependence on the initial rate which was similar to a Hinshelwood-Langmuir type of rate equation:

$$R = \frac{K_1 (P_{co})^2}{1 + K_2 (P_{co})^2}$$

where K_1 and K_2 are the reaction rate constant and the chemisorption equilibrium constant respectively. No effect on the reaction rate was found with varying flow rates of the gas.

The pressure dependence of the reaction on the initial rate was indicative of a chemisorption mechanism. Bulk gas diffusion did not appear to be a factor since varying gas flows did not effect the rate in these controlled experiments. The flow rates used were generally low ranging up to a liter per minute. The existence of other rate controlling steps besides the initial adsorption and surface reaction was indicated by the increasing activation energy as the reaction progressed. Generally, the studies showed that diffusion, either surface or bulk, of carbon is the controlling mechanism during the latter stages of the reaction.

Several investigators have found that the addition of up to 5 percent hydrogen can increase the amount of carbon deposition by as much as 100 times (68, 77, 78). The hydrogen effect is thought to be related to regeneration of active iron from inactive iron carbide.

Studies have been carried out on the reaction of carbon monoxide over bulk thin films and single crystals of iron to establish the sequence of the carbon monoxide reaction on iron (66, 80, 81, 82). These studies clearly eliminated the existence of any metal bearing liquid or gas phase intermediates. The reaction was verified as starting with adsorption,

then catalytic decomposition of carbon monoxide. The actual catalytic species has been much disputed (77, 78, 79, 81, 82) and the question is still probably not fully resolved. The active species is usually identified as iron or an oxide or iron. Cementite has been found generally to be inactive for this reaction. It has been well established (80, 81) that carbon does not initially build up or even exist in the free form on the surface. After decomposition of the carbon monoxide, the released carbon is absorbed into the surface. Ratliff (80) found that as saturation built up, decoration of grain boundaries, sub-grain boundaries, and dislocations were observed. Cementite (Fe_3C) was the first phase precipitated in the thin films and on the surface of 100 oriented iron single crystals. The growth of the cementite particles was shown to be controlled by the diffusion of carbon in the iron lattice and on the surface. The nucleation and growth of the cementite could be fully explained by the continuous precipitation theory.

Once the cementite reaches a critical volume at the surface, it decomposes to iron and carbon. Generally the carbon was observed in two typical forms, bulk or lamellae and filaments. The filaments were reported to have diameters in the range of 0.01 to 0.5 microns (79, 81, 83, 84, 85, 86). These filaments were found to contain small amounts of iron or carbides of iron (66, 69, 81, 82). Both types of carbon were generally graphitic in form and were believed to result from carbide decomposition (79, 80, 81, 82, 87, 88).

With the onset of carbon evolution and the presence of finely divided iron in the decomposition products, a large increase in the reaction rate occurs. This results in a very rapid deterioration of the supersaturated iron surface in the neighborhood of the cementite particle

producing graphite reaction products containing finely divided particles of iron and iron carbide.

The reaction maximum in iron and iron base alloys can be explained on the basis of the relative stability of the carbides involved. Alloying iron with chromium decreases the reactivity markedly with a slight increase in the temperature where the maximum reactivity for the alloy occurs.

The inhibiting effects of sulfur, ammonia, and water vapor in the gas stream in amounts from 0.01 to 0.5 percent have been studied (67). Sulfur additions in the form of H_2S were the most effective in decreasing the reaction in iron base materials and water vapor was effective for stainless steel inhibition. It appears that sulfur poisons the catalytic activity of the carbon monoxide decomposition on iron. It saturates adsorption sites and precipitation sites for carbide in the iron matrix and also substitutes for carbon in the Fe_3C lattice and makes it more stable. The effect of forming stable thermodynamic films on the surface was also found useful. In stainless steels and high chromium and silicon steels, preoxidation at low partial pressures of oxygen was found to be an effective deterrent to a catastrophic attack.

In summary carbon monoxide "metal dusting" attack on iron proceeds through the following steps (67):

A. Adsorption of carbon-monoxide.

B. Breakdown of carbon monoxide, the Boudouard reaction ($2CO \rightarrow CO_2$ + Carbon). This is probably rate controlling in the initial stages of the reaction.

C. Absorption of carbon into the surface by diffusion. This is rate controlling in the latter stages of the reaction.

D. Buildup of carbon in the solid solution and decoration of dislocations and sub-grain boundaries with carbon.

E. Precipitation of cementite at areas of higher carbon concentration.

F. Growth of cementite without other forms of carbide formation.

G. Having reached the critical concentration of cementite in the ferrite matrix, the cementite decomposes, regenerating carbon and iron plus the precipitation of subcarbides.

H. The deterioration of the base metal occurs by the continued precipitation of graphite with the growth of the decomposition products.

CHAPTER III

EXPERIMENTAL METHOD AND PROCEDURE

Generally speaking, an iron surface can affect the reaction of n-butane in two ways. The wire may alter the rate and the distribution of the products of n-butane pyrolysis, and also the iron surface may react with n-butane forming carbides and catalyzing the formation of carbon or graphite. In this work these two effects were investigated using two different experimental methods. To determine the effect of iron wire on the pyrolysis of n-butane, a low pressure pyrolysis technique was used. The extent of the reaction and the reaction products were monitored by mass spectrometry. The reaction of iron surfaces with the decomposition of n-butane was investigated in a quartz tubular flow reactor packed with iron wire. Carbon formation and metal deterioration were measured gravimetrically over the temperature and time ranges of interest and the wire surfaces were examined metallographically and with a scanning electron microscope. In addition, the equilibrium composition of the n-butane pyrolysis was calculated using a free energy minimization technique.

Low Pressure Pyrolysis

Method

The experimental technique of low pressure pyrolysis, first described by Benson and Spokes (89), consists of permitting a steady state flow of reactant molecules to pass into a thermostated reaction cell

under conditions of such low pressure that most collisions of reactant or product molecules take place with the vessel walls and not in the gas phase. Therefore, energy transfer from an external heat source is primarily by means of gas-wall interactions. Gas flow is free molecular flow. For the reactor used in this study this condition existed at a pressure of 10^{-2} mm. Once in the cell, the reactant molecules may decompose or escape from the cell. In quartz vessels, the rates of heterogeneous reactions are small but this is not necessarily the case in metal vessels (90). The reactant and product molecules are pumped from the reactor into a mass spectrometer for analysis.

For a reaction cell where the exit-aperture diameter is small compared with the tube diameter and the mean free path for gas-gas collisions is greater than the mean free path for gas-wall collisions the reactor will be a stirred flow reactor with very efficient self-stirring. It can be shown (see Appendix A) that for this reactor K, the first order overall rate constant of n-butane decomposition, is directly proportional to K_e, an escape rate constant of n-butane from the reactor which can be calculated from kinetic theory, and a ratio of the mass spectrometer signal when no reaction takes place to one when reaction occurs. That is:

$$K = K_e \frac{I^o - I}{I}$$

where

K = first order rate constant

K_e = escape rate constant

I° = mass spectrometer signal with no reaction

I = mass spectrometer signal with reaction

K_e (see Appendix A) is just a function of the shape of the vessel and the mean molecular speed of n-butane. For this experiment $K_e = 0.442\ T^{\frac{1}{2}}$ sec^{-1}.

To make a measurement, the mass flow rate is kept constant and the temperature range is scanned. At low temperatures where no reaction takes place we observe an output signal of the mass spectrometer I° at the parent peak of n-butane. At higher temperatures where reaction takes place we can observe the same peak I, which is now smaller since the signal is proportional to the flux of n-butane, and thus measure K directly from the ratio of peak heights. Also the entire spectrum can be scanned at reaction temperatures and compared to the low temperature no reaction spectrum to determine the nature of the reaction products.

This technique is good for determining the primary process in a pyrolytic system, since pyrolyses are carried out at pressures so low that secondary reactions are either eliminated or minimized. It has a disadvantage in that energy transfer to the molecules limits the rate of decomposition in many cases and thus the reaction rate constant can show a considerable fall off from the high pressure value.

This method was used to measure the effect of iron on the pyrolysis of n-butane. The pyrolysis was first carried out in a quartz reactor and then in the same reactor packed with various amounts of iron wire. The reaction rate and product distribution of these pyrolyses were then compared.

Apparatus

The n-butane used for the pyrolyses was instrument grade supplied by Matheson Gas Products. The gas had a minimum purity of 99.5 percent and was supplied in a lecture bottle under 16.3 psig pressure. The gas passes from the lecture bottle through a Granville-Phillips' variable leak valve and into a horizontal quartz reactor. The valve is connected to the reactor by a 24/40 Vycor ground glass joint. The pyrolysis takes place in a cylindrical quartz tube reactor approximately 25.4 cm long and 2.3 cm I.D. At the exit the quartz tube necks down to an aperture of 0.75 cm I.D. and 3.8 cm long. At 5.1 cm up from the exit aperture a 0.8 cm O.D. thermocouple well extends from the wall of the reaction chamber down the center of the reactor towards the entrance for 10.2 cm.

Heating is by means of four Lindberg Hevi-Duty type 73-KS clam shell heaters which provided a heated zone approximately 20.3 cm long. A chromel-alumel thermocouple with the hot junction placed in the center of the thermocouple well and the cold junction in ice water was used as the temperature control thermocouple. The thermocouple limits of error as set by the manufacturer are $\pm$ 0.75 percent. Standards of boiling distilled water and melting potassium bromide were used to verify this accuracy. A Leeds and Northrup portable precision potentiometer was used to measure the thermocouple potential during this test. Details are given in Table 1. The controller used during pyrolyses is a Leeds and Northrup Speedomax H Continuously-Adjustable AZAR Recorder and Controller wired for on and off control. The temperature as measured by the central thermocouple was controlled to $\pm$ 5°C by the controller. The heaters were surrounded by fire bricks to reduce drafts and to insulate from heat

losses at higher temperatures. It was necessary to cool the ground glass joint at the entrance of the reactor to maintain vacuum. This was done with an air blast and has led to some cooling of the reactor near the beginning of the heated zone. However, a few centimeters into the heated zone temperatures were generally within $\pm$ 10°C of the central temperature.

Table 1. Thermocouple Verification

Standards Used for the Chromel-Alumel Thermocouple		
Boiling Water:	Recorded Temperature	99.5°C
	Actual Water Temperature	99.3°C
	Atmospheric Pressure	740.4 mm
Melting Potassium Bromide:	Melting Point	730.0°C
	Recorded Melting Temperature	730.7°C

The reactor connects into a 1.5 inch copper tubing tee. The vacuum seal is maintained by an O-ring glass to metal pressure seal similar to a Cajon connector. The vertical run of the tee connects to a Vaco 1½" in-line valve and then to a roughing pump. The horizontal run of the tee also connects to the same type of in-line valve. These valves were used to isolate the reaction chamber when necessary and then to rough pump the chamber without breaking the vacuum of the mass spectrometer. The horizontal valve connects by an O-ring flange to 3" O.D. type 304 stainless steel tee. The vertical run of the tee connects to a low pressure pumping system consisting of a CVC 4" Gate Valve, a CVC 4" liquid nitrogen

cooled cold trap, a CVC 4" three stage oil diffusion pump, and a Cenco Megavac forepump. This pumping station was used to aid the system attached to the mass spectrometer in order to pump down the reaction chamber to a base pressure within a reasonable time. After the base pressure was reached the pumping system was isolated from the reaction chamber by the gate valve.

The horizontal run of the stainless steel tee is connected by an O-ring flange directly to the ion source vacuum chamber of a Bendix Model 14-107 Time of Flight Mass Spectrometer, which has been described in the literature (91). The output from the analog scanner is recorded on a Hewlett Packard 7001 AR X-Y recorder. The recorder had a stated accuracy of 0.2 percent of full scale. The pressure was monitored by thermocouple gauges on the roughing lines of the reaction chamber and and mass spectrometer. Pressure down to 1×10^{-6} mm was monitored by a Veeco cold cathode discharge gauge located on the flight tube of the mass spectrometer. Figure 3 is a photograph of the inlet system and the mass spectrometer.

The iron wire used in the pyrolysis was Leeds and Northrup iron thermocouple wire AWG number 28 which has a diameter of 0.051 cm. A spectrographic analysis, shown in Table 2, determined that the purity exclusive of gases was greater than 99.8 percent.

a.

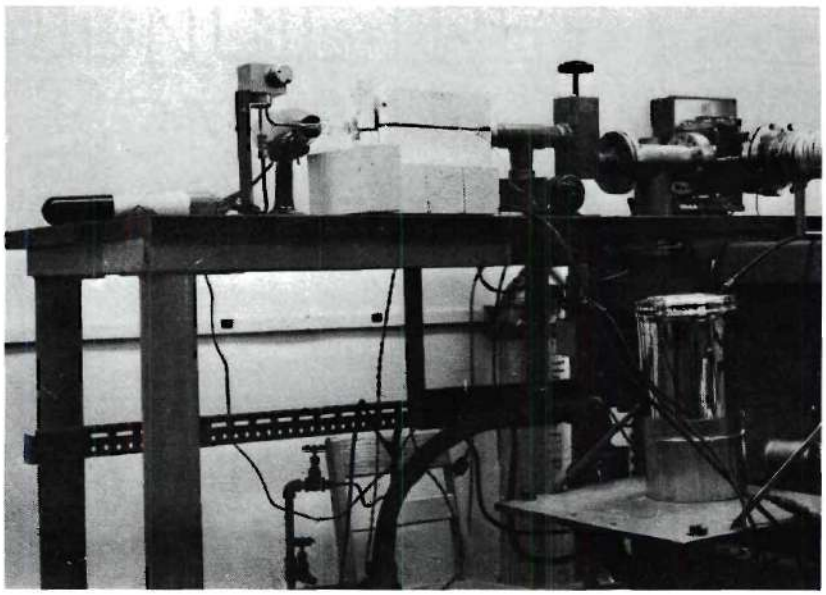

b.

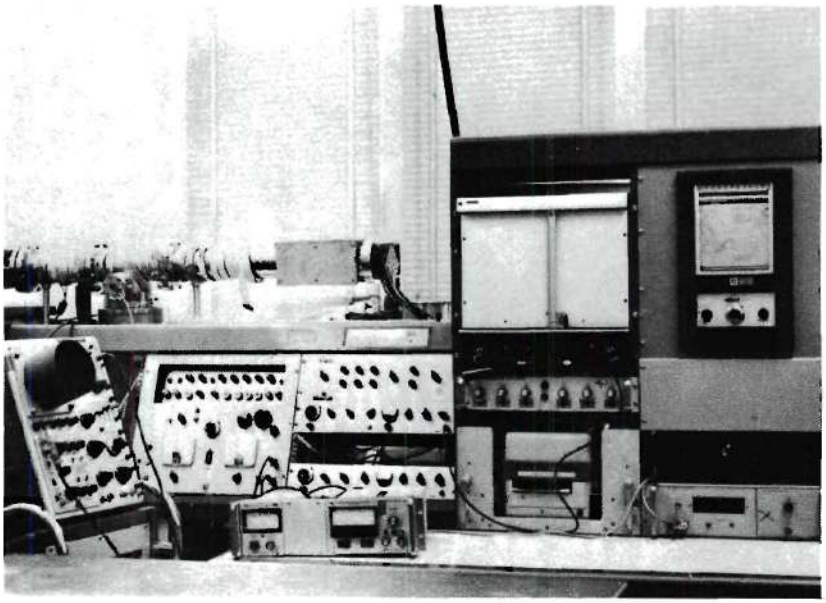

Figure 3. Low Pressure Pyrolysis Apparatus, a) Inlet System, b) Mass Spectrometer.

Table 2. Laboratory Spectrographic Analysis of Iron Wire

	Weight %		Weight %
Carbon	0.014	Nickel	0.019
Manganese	0.016	Chromium	0.005
Sulfur	0.018	Cobalt	0.0001
Phosphorous	0.017	Copper	0.092
Silicon	0.002	Molybdenum	0.002
Iron	Balance		

Procedure

The reaction chamber was pumped to a base pressure of about 1×10^{-6} torr with both pumping systems. Then the auxiliary pumping system was valved off and all further pumping was through the source of the mass spectrometer by its pumps. The mass spectrometer pumps had no trouble maintaining the base pressure once it was reached. A slight air leak gave peaks at 28 and 32 amu and residual gases, mainly water, gave interference at 17, 18 and less importantly at other places in the mass spectrum. A correction was applied when interference occurred. The background spectrum was always small in comparison with the spectrum of the reacting gases and never posed any serious interference problems.

The n-butane was passed through the adjustable leak valve at a rate of about 4×10^{14} molecules/sec. The flow rate was adjusted so that the base pressure in the mass spectrometer did not rise above 2×10^{-6} mm. When the valve was first opened it took about an hour to obtain a spectrum with constant peak heights.

The pressure in the reaction chamber was estimated to be about 2×10^{-4} mm. At that pressure and room temperature, n-butane has a mean free path of approximately 11 cm. The average residence time of n-butane in the reactor is the reciprocal of K_e and averaged about 0.065 sec. The ratio of internal surface area to exit aperture area gives the average number of gas-wall collisions made by a molecule while in the reactor. In these experiments this ranged from 300 to 650 depending on the amount of packing.

After steady state flow had been reached, the output from the parent peak of n-butane, 58 amu, was recorded on graph paper by an X-Y recorder at room temperature. This particular peak of the n-butane spectrum was chosen since there would be no chance of interference between it and the lower molecular weight pyrolysis products. During the pyrolyses there was no detection of higher molecular weight products. This indicated that no polymerization was taking place during the reactions. The peak height was taken as the average value over ten graph divisions which took about 30 seconds to record. The variation during recording was usually very low, amounting to less than 1 percent of the total peak height.

All experiments were carried out at a constant ionizing voltage of 70 volts and an electron trap current of 0.125 microamperes. When a single peak was monitored a large gate width and a time constant of 0.5 seconds was used to insure good stability. When the spectrum was scanned a smaller gate width and a time constant of 0.05 seconds was used to insure good resolution. The range of the X-Y recorder was kept constant at 2 volts per inch and a sweep rate of 20 seconds per inch. Output adjustments

before an experiment to insure a full scale measurement were made with the analog's variable scan rate and scanner multipliers.

After recording peak height at room temperature where no reaction took place, the reactor was heated to a particular reaction temperature for study and the same peak height measured. From a ratio of the peak heights with and without reaction, the rate constant K was determined. Before a reading was made at the temperature under study, the temperature was maintained for about fifteen minutes in order to obtain short term reproducibility of the output signal. This was done mainly for the temperature controller to smooth out fluctuations in temperature.

The reactor was then cooled and the peak height recorded again when no reaction occurred. Because there were occasional problems with the peak height drifting during an experiment, usually only one or two temperature data points were recorded per furnace heating. The data was accepted only if the base peak heights which were recorded before and after heating to the reaction temperature corresponded.

As a result of the distance from the reaction chamber to the ion source, the product gases have made many collisions with the walls of the inlet system and have thus cooled to room temperature by the time they reach the ion source. However, the distance between the reaction chamber and the source did not cause any measurable time lag between introduction of the gas and appearance of the mass spectrometer signal. Also, adsorption of the gases in the system did not present a problem. When the gas flow was interrupted the residual spectrum was very small.

The entire spectrum was scanned several times when no reaction was occurring and during the reaction. This was done both for the empty

reactor and also during the pyrolyses at the various packing conditions of the reactor.

Each individual data point reported is an average of five separate determinations. Data were determined from 850°C, where the reaction was first measurable, in 50°C intervals up to 1050°C. Four different reactor conditions were examined. These included an empty reactor, the reactor packed with iron wire having a surface area of 50 and 200 cm^2 and also the reactor packed with 0.7 cm O.D. quartz tubing have a surface area of 200 cm^2. Details of the reactor conditions are given in Table 3.

Table 3. Reactor Conditions

Packing Conditions	Surface/Volume (cm^{-1})	% Reactor Surface of Iron
Empty	2.24	0.0
200 cm^2 Quartz Tube	5.15	0.0
50 cm^2 Iron Wire	2.82	25.8
200 cm^2 Iron Wire	5.15	56.5

The wire used was received from the manufacturer wound on a two inch spool. It was stored under a light lubricating oil until ready for use. When ready for use the wire was cleaned with tricloroethylene. The wire was then cut to the required size and wound into spring-like coils. The coils were then cleaned further by successive soakings in tricloroethylene, acetone and absolute ethyl alcohol. The coils were then packed into the reactor around the thermocouple well. The reactor was packed with fresh wire for each condition of packing studied.

Tubular Flow Reactor

Method

To investigate the reaction of iron surfaces during the pyrolysis of n-butane a quartz tubular flow reactor packed with iron wire was used. The reactor was essentially at atmospheric pressure and heated by a tube furnace. Carbon formation on the wire and metal deterioration of the wire were measured gravimetrically. The wire itself was examined metallographically. The carbon deposits growing from the wire surface were examined with a scanning electron microscope.

Apparatus

The n-butane used for the pyrolysis was C.P. grade supplied by Matheson Gas Products. The gas had a minimum purity of 99.0 percent. The gas was regulated from the cylinder by a two stage gas regulator. Argon, which was used as an inert atmosphere during heating and cooling of the reactor, was supplied by Gas Products and had a minimum purity of 99.995 percent. The gas was removed from the cylinders through the regulators to a manifold which connected directly to an Airco Model 09-1021 rotameter. The rotameter was calibrated for n-butane. The gas handling system was constructed of 0.25 inch O.D. copper tubing. The outlet of the rotameter connects directly to a 24/40 ground glass joint by Tygon tubing and the joint mates to the entrance of the tubular reactor.

The reactor is a quartz tube with a 2.3 cm inside diameter and a length of 57.8 cm. The gas exhausts from the reactor through a 24/40 ground glass joint connected with tygon tubing into a hood. Heating and temperature control was done by a Lindberg Hevi-Duty Single Zone Tube Furnace and Controller model numbers 54031 and 59349, respectively. The

furnace had a heating zone of 30.5 cm and the temperature was monitored by a Platinel II thermocouple placed at the center of the heating zone. The controller was able to maintain an accuracy of $\pm$ 1°C at the thermocouple. Figure 4 is a photograph of this reactor system. The iron wire used was Leeds and Northrup iron thermocouple wire with a purity of greater than 99.8 percent.

Procedure

The iron wire used for the experiment was the same as that used in the pyrolysis experiment. It was received wound on a two inch spool and stored under a light lubricating oil until ready for use. Each sample consisted of 62.7 cm in length of the 0.051 cm diameter wire. This length of wire gave a surface area of 10 cm^2. The wire was cut to length and wound spring-like into a coil about 1 cm in diameter and about 1 cm long. Before coiling, the wire was wiped with tricloroethylene to remove the oil. After coiling the wire was further cleaned by successive soakings in tricloroethylene, acetone, and absolute ethyl alcohol. The sample was then weighed on a Mettler analytical balance, model H-10, to the nearest 0.1 mg. The sample was then placed in the quartz reactor at the center of the heated zone directly beneath the furnace thermocouple. The furnace was then heated to the temperature in question while a steady flow of inert argon gas flowed through the reactor. When temperature had been reached the argon flow was shut off and n-butane flowed into the reactor through the rotameter. The majority of the experiments were done at the same flow rate of 48.9 cc/min. Small variations of the flow rate were found not to have a significant effect on the results. The average residence time of the gas in the heated section of the reactor was 2.37 minutes.

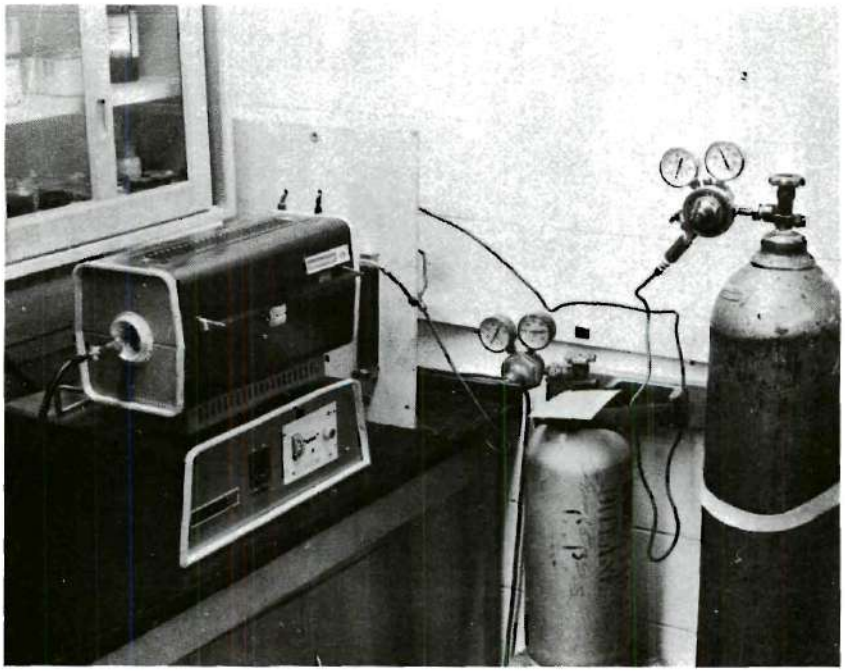

Figure 4. Tube Flow Apparatus.

After the reaction the sample was cooled to room temperature in the furnace again under the flow of argon.

After cooling the sample, the wire and all carbonaceous deposits were removed from the reactor and weighed. Any carbonaceous deposits on the wire were then removed by wiping with acetone and the samples reweighed. The samples were then cleaned with an ultrasonic cleaner, wiped with acetone and reweighed. This was continued until a constant weight was found.

Data were taken beginning at 595°C where dusting and metal deterioration first showed up in a 20 hour reaction period. The temperature was increased in approximately 50°C intervals and data taken at 642°C, 689°C, and 737°C and 786°C. At each temperature data were taken for times of 1, 2, 4, 8, 16, and 20 hours. Each value reported is an average of three different determinations.

Analysis of the Wire

Representative samples were chosen to be examined optically by standard metallographic techniques. Samples were mounted in Quickmount, wet-ground on the standard papers and polished on a lap wheel with chromium oxide. At first problems of rounded edges which prevented observation of the important surface area occurred. This was solved by the addition of a mounting filler, Buehler No. 20-8148 80 Mesh, in the Quickmount which resulted in even grinding, prevented much of the edge rounding and permitted much better observation of the sample. A nital etch was used which consisted of 2 percent nitric acid in absolute alcohol. This etch reveals the ferrite boundaries and darkens the pearlite.

Several samples, many still with carbon deposits, were examined with a scanning electron microscope. This technique has the advantage

of very good resolution (150 A) and exceptional depth of focus (about 300 times that of an optical microscope). In the scanning microscope a specimen is bombarded with high energy electrons and thus emits backscattered electrons, secondary electrons, and x-rays. Secondary and backscattered electrons provide information about surfaces. High energy backscattered electrons move from the sample to the collector in a straight line. The lower energy secondary electrons follow a curved path to the collector and reveal details of holes and crevices. The electron beam is accelerated from 20 to 25 Kv. Condenser and objective lenses focus the beam on the specimen surface from which electrons are emitted. Electrons collected in the detector comprise a signal which is amplified and displayed on a cathode ray tube. Photographs of the image as displayed on the cathode ray tube are then taken.

Equilibrium Calculations

Thermodynamic calculations were made of the equilibrium composition of the pyrolysis products of n-butane. The Gibbs free energy minimization technique of White, Johnson and Dantzig (93) and its extension to include the presence of condensed phases by Kubert and Stephanous (94) was used. An Algol computer program was written to make the calculation. This method directly minimizes the Gibbs free energy of a system containing any number of gas species and condensed species as long as one is consistent with the phase rule. Each gas species is considered ideal and each condensed species is considered as a separate and pure phase. In this computation a species was considered not present at equilibrium and not considered further in the calculation when the amount present fell below 1×10^{-9} mole. The assumed starting composition was usually

about twenty-five moles, although the number of moles present did not affect the final equilibrium composition. Equilibrium was assumed to be attained when the difference in free energy between the last computation and the next to last computation was less than 1.0×10^{-8} cal.

Fifteen gas species were considered as possibly present at equilibrium. This included n-butane, and all carbon-hydrogen compounds with four or less carbon atoms plus hydrogen. The assumed starting composition gave a C:H ratio of 4:10 which is that of n-butane. In addition, duplicate runs were calculated which also considered that the condensed specie, carbon as graphite, was present at equilibrium. The thermodynamic data, free energy function and heat of formation of each compound, were taken from the API Research Project 44 (95). Pressures and temperatures used in the calculations corresponded to the pressures and temperatures of the experimental work.

CHAPTER IV

RESULTS AND DISCUSSION

The objective of the experimental program was to measure the kinetics of the n-butane "metal dusting" reaction with iron in order to determine, if possible, a mechanism for the reaction consistent with the data. This hydrocarbon reaction was then to be compared with the known kinetics of carbon monoxide "metal dusting" to determine if the reactions were proceeding through the same type of mechanism and to gauge the relative importance of these two types of "metal dusting" reactions.

The study of the reaction of n-butane over iron presents some problems not present with the carbon monoxide reaction. Carbon monoxide will decompose between 450° and 800°C, the usual metal dusting temperatures, only in the presence of a catalyst. However, n-butane will decompose and, depending on the reaction conditions, polymerize homogeneously in the "metal dusting" temperature range. Furthermore, with increasing temperature, reaction thermodynamics restricts carbon monoxide decomposition, but enhances n-butane decomposition. Thus with n-butane one has the added complication of a homogeneous reaction preceeding simultaneously with the heterogeneous "metal dusting" reaction.

Two different experiments were conducted to determine the kinetics at different stages during the reaction. The tube flow reactor measured the reaction of iron wire during the n-butane decomposition. The weight of carbon formation and weight loss of the iron wire were measured for various times and temperatures. This method shows the final results of

the reaction on the iron wire. There is also a considerable amount of this type of data for the carbon monoxide "metal dusting" reaction which can be used for comparison. The low pressure pyrolysis reactor measures the effect of iron wire on the kinetics of n-butane decomposition. The reaction rate constant and the product distribution are measured in the reactor with and without iron wire packing. This method in effect measures the interaction of iron and n-butane in the early stages of "metal dusting" reaction before carbon formation occurs. The differences in the rate constants was due entirely to the effect of the iron surface area on the decomposition of n-butane. The equilibrium composition of the n-butane decomposition was also calculated to determine if there were any thermodynamic restrictions placed on this reaction.

Equilibrium Calculations

The equilibrium composition for the n-butane decomposition was calculated from 500° to 1000°C at 100°C intervals. Calculations were carried out for pressures of 760 mm and 1×10^{-4} mm. The equilibrium composition was determined for the condition that only a gas phase was present and then repeated allowing for the formation of solid carbon along with the gas phase. In all cases the system that allowed for carbon formation had a lower free energy at equilibrium than the comparable gas phase system and thus was the true equilibrium system. However, in cases where kinetics do not permit carbon formation the pseudo-equilibrium of the gas phase system is probably the limiting composition.

Figures 5 through 8 show the results of these calculations. For the low pressure systems at all temperatures acetylene and hydrogen are the only species present for the one phase system and carbon and hydrogen

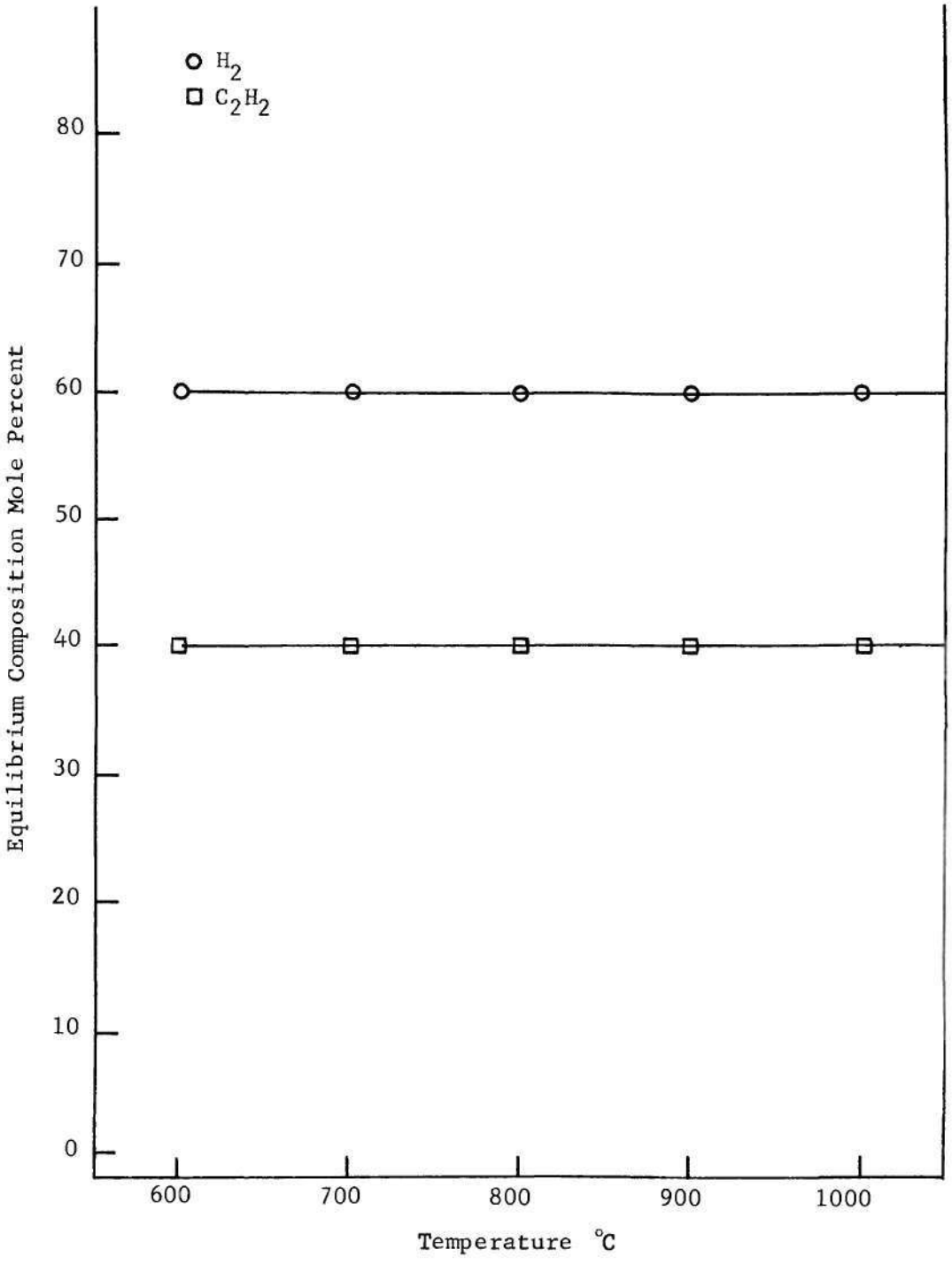

Figure 5. Equilibrium Composition of the n-Butane Pyrolysis at 1×10^{-4} mm Pressure with One Phase.

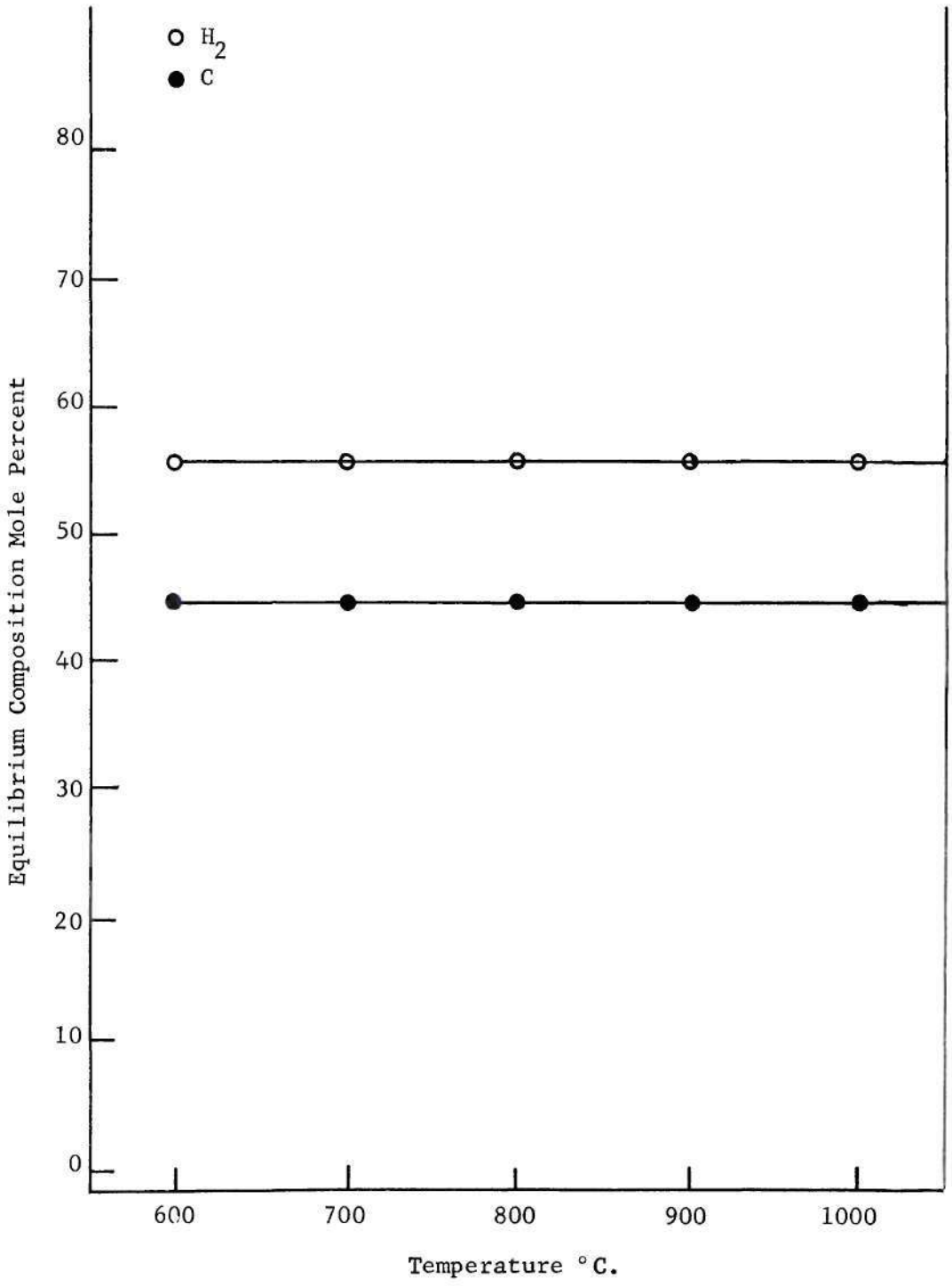

Figure 6. Equilibrium Composition of the n-Butane Pyrolysis at 1×10^{-4} mm Pressure with Two Phases.

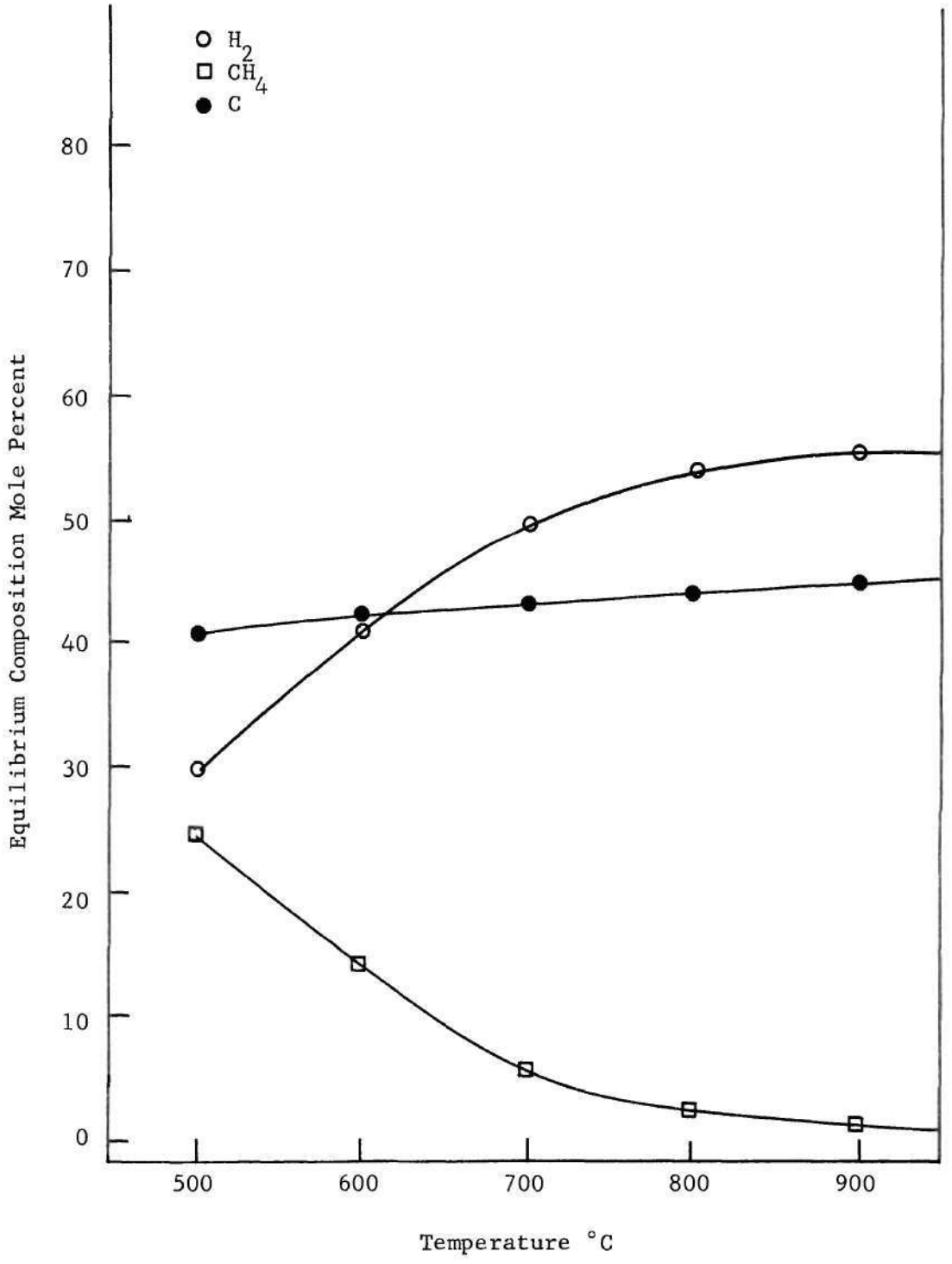

Figure 7. Equilibrium Composition of the n-Butane Pyrolysis at 760 mm Pressure with Two Phases.

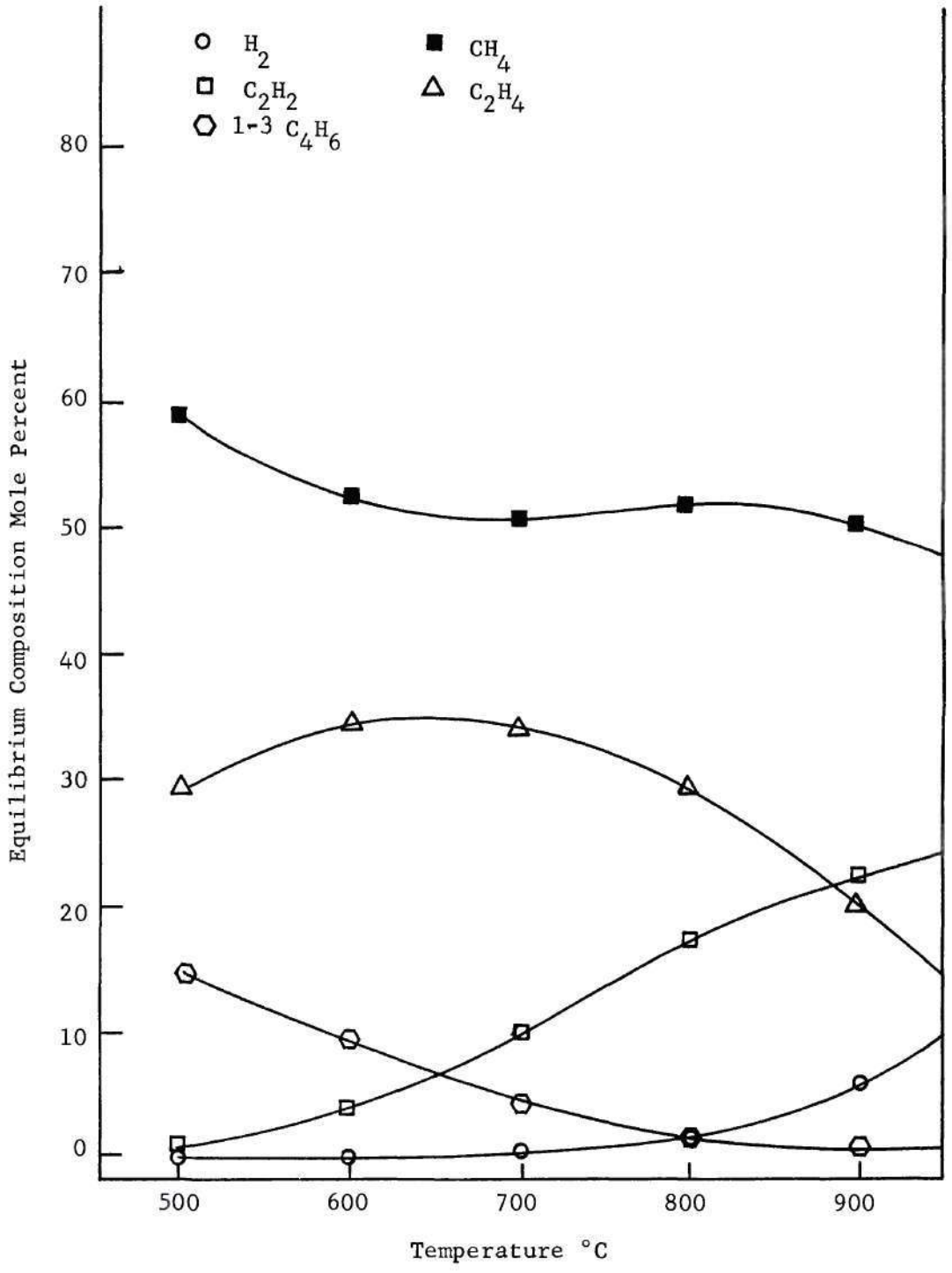

Figure 8. Equilibrium Composition of the n-Butane Pyrolysis at 760 mm Pressure with One Phase.

for the two phase system. In the two phase high pressure system only hydrogen, methane, and carbon were present in more than trace amounts. The one phase high pressure system had several species present. It is interesting to note that for this system while 1-3 butadiene comprises an important portion of the equilibrium gas phase at the lower temperatures, it is not a product of the experimental decomposition of n-butane. The decomposition of n-butane proceeds by a free radical chain mechanism in which the chains are initiated by the splitting of the molecule at its weakest link, the carbon bond. Thus while thermodynamics favors the formation of 1-3 butadiene, the kinetics of the reaction are such that this specie is not formed.

Low Pressure Pyrolysis

Results

The extent of the decomposition of n-butane was followed by measuring the ratio of reactant peaks. From the kinetic equations for this system the first order rate constant was computed. Table 4 presents the percent of n-butane decomposition and the log of the reaction rate constant for the packing conditions and temperatures investigated. Also included is log K_∞ the high pressure values calculated from the Arrhenius parameters (3). Each value reported is an average of five determinations. The day to day reproducibility of the experiment was very good. The deviation of the experimental values from the reported value is no more than $\pm$ 5 percent except for the lowest temperature where it is about $\pm$ 10 percent.

Quartz packing was used to determine if the surface of the reactor was influencing the reaction. The results showed no significant difference

Table 4. Percent Decomposition and Reaction Rate Constant for the Low Pressure Pyrolysis of n-Butane.

Temperature (°C)	Reactor Packing	Percent Decomposition	Log K	Log K_∞
1050	Empty	40.0	1.03	3.07
	200 cm^2 Quartz	40.7	1.04	
	50 cm^2 Iron	47.0	1.16	
	200 cm^2 Iron	59.4	1.28	
1000	Empty	29.3	0.71	2.70
	200 cm^2 Quartz	23.4	0.68	
	50 cm^2 Iron	27.9	0.79	
	200 cm^2 Iron	33.3	0.90	
950	Empty	12.4	0.34	2.29
	200 cm^2 Quartz	12.5	0.35	
	50 cm^2 Iron	14.4	0.92	
	200 cm^2 Iron	17.3	0.51	
900	Empty	5.2	-0.09	1.84
	200 cm^2 Quartz	5.5	-0.05	
	50 cm^2 Iron	6.0	-0.01	
	200 cm^2 Iron	6.5	-0.03	
850	Empty	2.5	-0.43	1.36
	200 cm^2 Quartz	2.4	-0.44	
	50 cm^2 Iron	2.6	-0.40	
	200 cm^2 Iron	2.7	-0.39	

between the reaction rate constant of the packed and unpacked quartz reactor. Furthermore, the only conditioning effect found in the reactor was at the exit aperture. A slight discoloration of the reactor appeared at this point after a few experiments. This conditioning did not appear anywhere else on the reactor and after a few runs the conditioning at the exit aperture seemed to stop.

Rate constants are typically two orders of magnitude lower than the high pressure values for n-butane. For the unpacked reactor the fall off increased with temperature while the packed reactor tended to have a constant fall off. Figure 9 shows log K as a function of temperature for the different reaction conditions. Included for comparison is log K_∞, the high pressure value. Figure 10 is a plot of the percent of decomposition of n-butane versus the percent of the reactor surface which was iron at the different reaction temperatures. The increase in decomposition of the gas was proportional to the increase of iron surface in the reactor.

The most important reaction products were found at atomic mass units of 26, 27 and 28, with various other atomic mass units (amu) contributing lesser amounts. Table 5 shows the relative intensity of the product spectrum for the empty and packed reactor at 1050°C. Interference from the unreacted n-butane was subtracted from the spectrum and all values were made relative to amu 28 for the packed reactor. The main species which contribute to the spectrum at these mass units are the C_2 hydrocarbons, ethane, ethylene, and acetylene. The small amount of methane formed can be seen by a relatively small peak at amu 16. Propylene, whose main peak is at 41 is also not a major product. Table 6 gives the relative intensities of the packed and unpacked reactor for the amu 26,

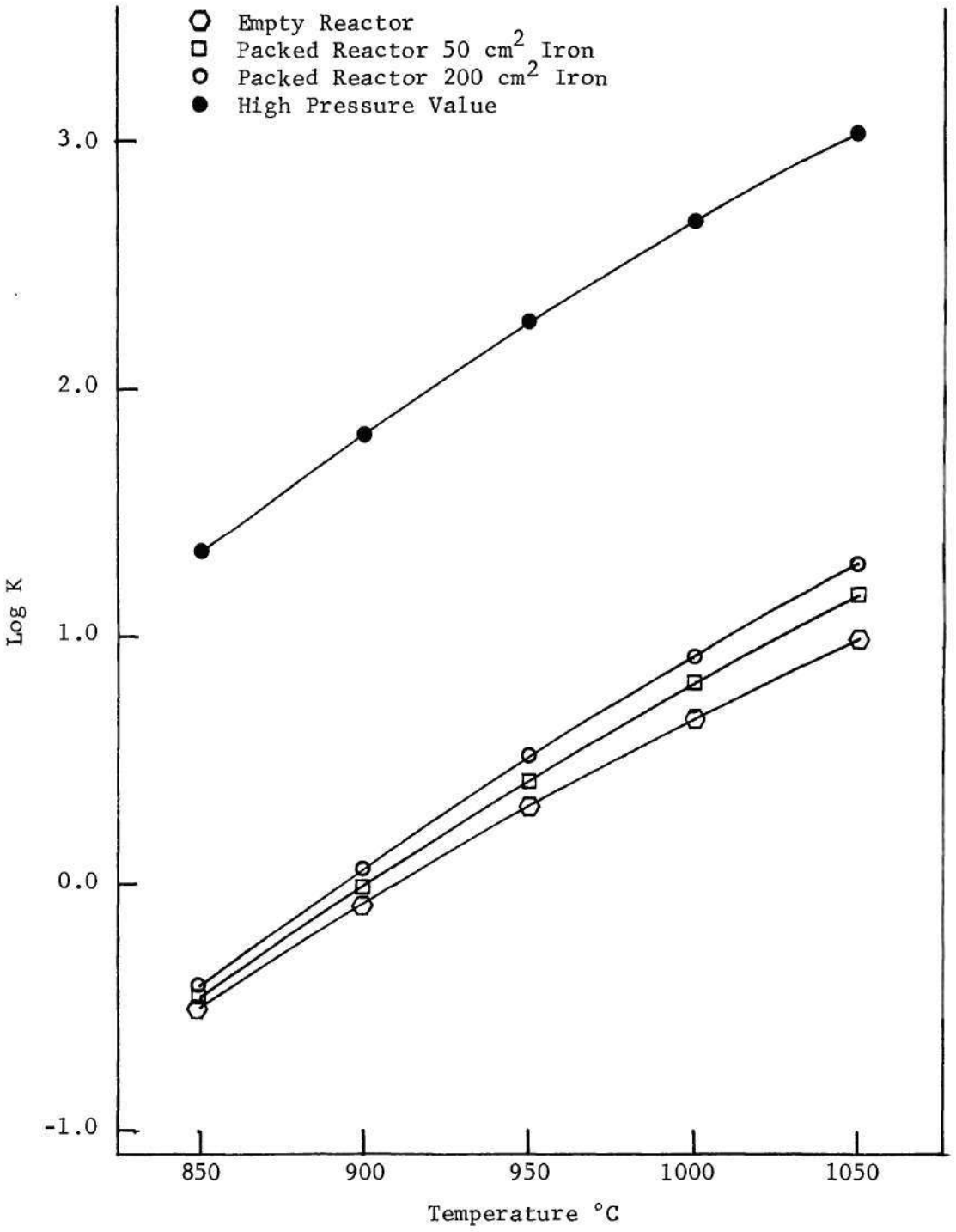

Figure 9. Log K versus Temperature.

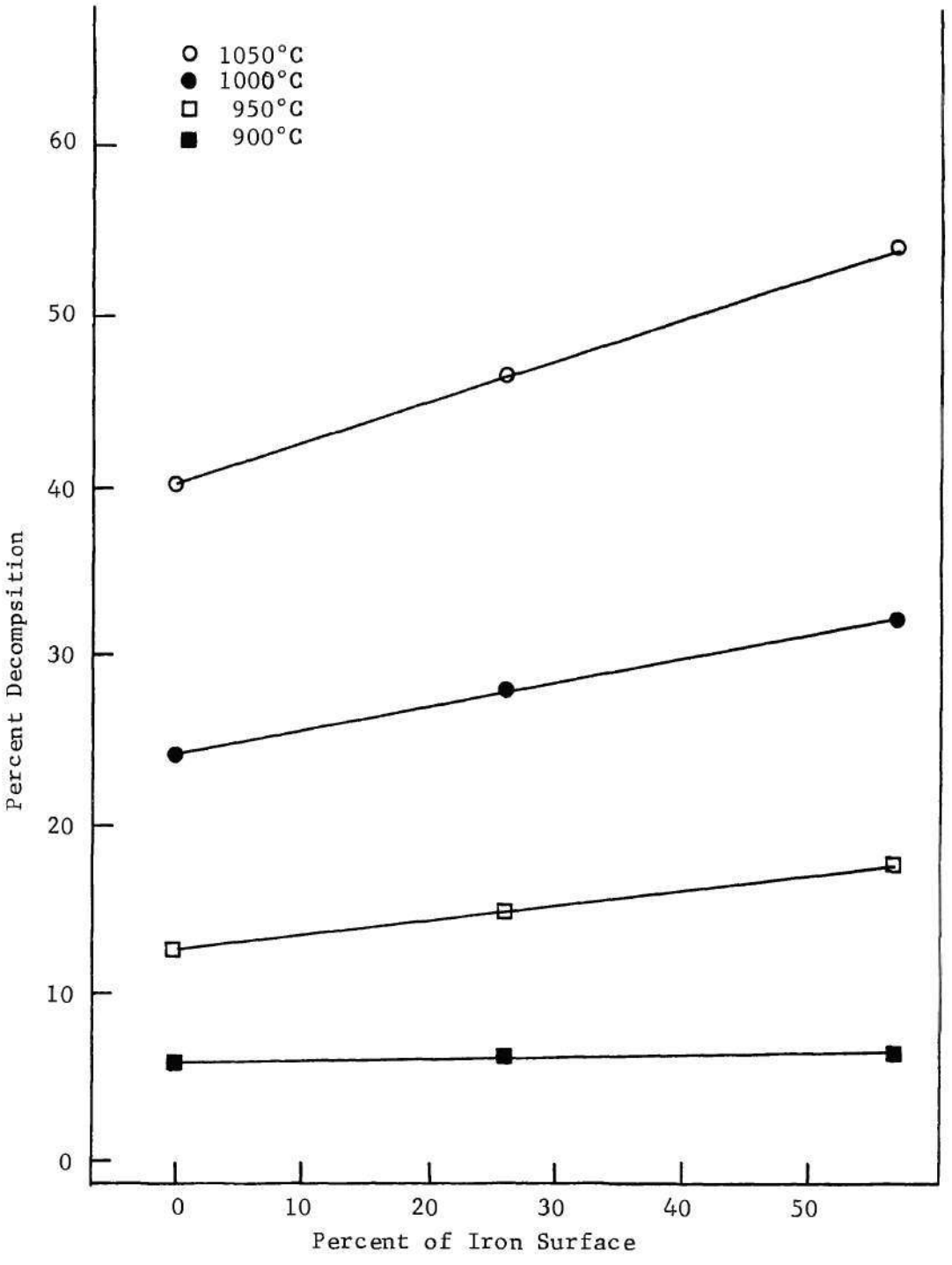

Figure 10. Percent of n-Butane Decomposition versus Percent of Iron Surface in the Reactor.

Table 5. Relative Intensities of the Product Spectrum

Atomic Mass Unit	Packing Condition		
	Empty	50 cm^2 Iron	200 cm^2 Iron
42	2.0	2.4	1.3
41	3.6	2.5	6.1
40	1.0	1.1	1.6
39	3.0	2.3	4.2
29	6.0	2.5	2.8
28	60.6	72.8	100.0
27	37.5	30.4	27.8
26	31.9	29.2	24.9
25	6.1	5.8	5.0
16	3.8	1.2	3.3
15	9.0	0.7	0.4
14	4.5	3.4	3.4

Table 6. Relative Intensities of the Product Species

Atomic Mass Unit	Compound or Packing Condition				
	C_2H_6	C_2H_4	C_2H_2	Empty	200 cm^2 Iron
28	100	100	-	100	100
27	29.3	64.8	2.8	61.9	27.8
26	18.2	62.3	100	52.6	29.9

27, and 28 in addition to the intensities for pure ethane, ethylene and acetylene. The data for the pure compounds were taken from API mass spectral data (95). For the unpacked reactor the reaction product was mostly ethylene. However, with iron surface area, the peaks at amu 27 and 26 become smaller, indicating the formation of ethane and some acetylene in preference to ethylene.

Discussion of Results

The iron packing catalyzed the decomposition of n-butane and increased packing enhanced the decomposition. At 1050°C with 200 cm^2 of surface the amount of decomposition increased by approximately 35 percent and the reaction rate constant almost doubled from the quartz reactor without iron packing. As seen from Table 4 quartz packing had no significant effect at all on the reaction and there was almost no sign of a conditioning effect of the quartz reactor itself. Thus the quartz surface for the relatively small s/v ratios investigated had no effect on the reaction. Other investigators have also found this to be true (16, 19, 20). However, increased iron surface enhanced the amount of decomposition of n-butane and this enhancement was proportional to the increase of iron surface in the reactor. This indicates that a surface reaction between the iron and the gas is occurring which leads to the increased decomposition.

No decomposition was detected in the packed or unpacked reactors until 850°C. The iron did not catalyze the reaction of the gas to a detectable extent until decomposition had begun.

Since the pressure was so low that most of the collisions of the molecules took place at the wall and since the quartz wall did not affect the reaction, the reaction was essentially unimolecular. Unimolecular reaction theory predicts a fall off in the rate constant at low pressures due to a decrease of activated molecules caused by collisions (96). Further this fall off should increase with increasing temperature (89). Table 7 shows the ratio of K_∞ , the high pressure rate constant, and K, the low pressure constant, for the unpacked reactor and the reactor

Table 7. The Ratio of the High and Low Pressure Rate Constants for the Empty and Packed Reactor.

Reactor Condition	Temperature (°C)			
	900	950	1000	1050
Empty	85	85	98	110
200 cm^2 Iron	65	60	63	62

packed with 200 cm^2 of wire. A higher ratio indicates a greater fall off. For the unpacked reactor the fall off does increase with increasing temperature as expected. However, the packed reactor shows an almost constant fall off. This suggests a departure from a unimolecular reaction with a purely heterogeneous reaction occurring.

Most of the reaction products were C_2 hydrocarbons. Since the pressure was so low in the reactor that there were very few gas-gas collisions, contributions by gas-phase bimolecular reactions can be ignored. If the bimolecular steps are eliminated from the accepted free radical chain mechanism for the pyrolysis of n-butane, the following steps would be left:

$$C_4H_{10} \longrightarrow 2C_2H_5\cdot$$

$$C_2H_5\cdot \longrightarrow C_2H_4 + H\cdot$$

$$C_4H_{10} \longrightarrow CH_3\cdot + 1 - C_3H_7\cdot$$

$$1 - C_3H_7\cdot \longrightarrow C_2H_4 + CH_3\cdot$$

This scheme predicts ethylene as the main product and in the unpacked reactor ethylene was the main product. Packing the reactor with iron wire caused a dramatic increase in the rate of reaction and a change in the product spectrum. Ethylene, ethane and acetylene were products of the packed reactor pyrolysis. The equilibrium composition of the gas at this pressure was calculated to consist of acetylene and hydrogen. The iron packing catalyzed the pyrolysis of n-butane by accelerating the rate in the direction of thermodynamic equilibrium. The exact mechanism of decomposition for this case is not certain. However, a surface precursor of the molecule or free radical which can dissociate or re-evaporate would be necessary to account for the product.

Tubular Flow Reactor

Results

The tubular flow reactor was used to measure the reaction of iron with n-butane. The quartz reactor was packed with 10 cm^2 of iron wire. As n-butane is passed over the wire at appropriate temperatures, carbon begins to appear, growing from the wire surface and forming deposits completely covering the wire. The carbon is in the form of a dust or powder which does not adhere very readily to the metal surface. Figure 11 shows a typical reacted wire with the carbon formed on the surface at 642°C. Along with carbon formation the metal surface undergoes general pitting and surface wastage. Without iron in the reactor tube there is no carbon deposited.

The carbon formation and metal deterioration were monitored gravimetrically for times up to twenty hours in the temperature range of the reaction. Each value reported is an average of three different

Figure 11. Reaction Products After Twenty Hours at 642°C.

determinations. The reproducibility of the data was reasonably good. The average deviation from the mean value reported for all experiments was 13.9 percent. The maximum deviation was 38.0 percent. Table 8 presents this data for the times and temperatures investigated.

Figures 12, 13 and 14 are plots of the weight of the carbon deposited and the weight loss of iron wire versus time for the temperatures investigated. These curves show that after an initial transient period of slow or no reaction there is a short period of rapid weight gain or loss followed by a slower change of weight with increased time. The initial incubation period decreased with increasing temperature and was less than one hour for temperatures at 642°C and above. The rapid reaction period lasted for approximately an hour.

The slope of the weight gain and loss curve is a measure of the rate of carbon formation and metal loss respectively. After the initial phases of the reaction this slope is constant. Table 9 shows values of K, the rate constants for the weight loss and gain curves. These K values were each determined by a least squares fit of a line to the data points. From an Arrhenius plot of the rate constant an activation energy of 36 Kcal/mole was found for weight loss and 50 Kcal/mole for weight gain.

Figure 15 is a plot of the weight of carbon deposited versus the weight of metal loss at the temperatures investigated. The correlation between the two at a given temperature is very good. As the temperature increases the slopes of these lines decrease. At lower temperatures much more weight is lost per gram of carbon deposited.

The first signs of a reaction on the iron wire within 20 hours appeared at 595°C with a small amount of carbon dust formation on parts

Table 8. Weight of Carbon Formation and Weight Loss of Iron Wire in the Tube Flow Reactor.

Temperature °C		595	642	689	737	786
Time/Hr.						
1	wt. gain gm	0.000	0.019	0.044	0.001	0.003
	wt. loss gm	0.000	0.002	0.001	0.000	0.000
2	wt. gain gm	0.000	0.110	0.650	2.158	0.008
	wt. loss gm	0.000	0.007	0.023	0.028	0.000
4	wt. gain gm	0.000	0.466	1.504	2.944	0.017
	wt. loss gm	0.000	0.032	0.035	0.033	0.000
8	wt. gain gm	0.001	1.529	3.048	4.237	0.018
	wt. loss gm	0.000	0.040	0.057	0.040	0.000
15	wt. gain gm	0.004	1.863	5.351	6.655	0.034
	wt. loss gm	0.000	0.049	0.100	0.055	0.000
20	wt. gain gm	0.013	2.493	6.494	8.493	0.045
	wt. loss gm	0.002	0.063	0.113	0.067	0.000

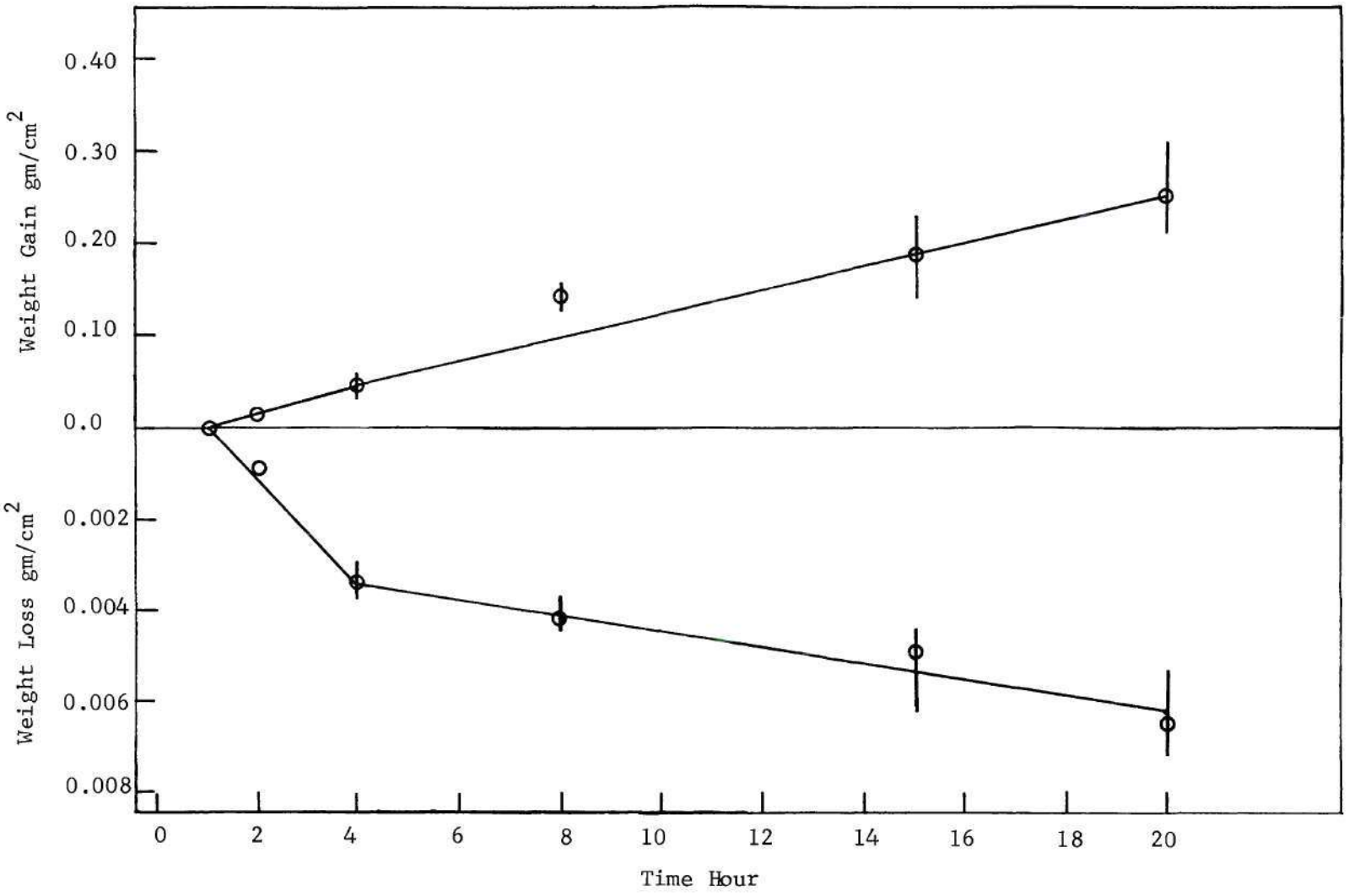

Figure 12. Weight Gain and Loss versus Time at 642°C.

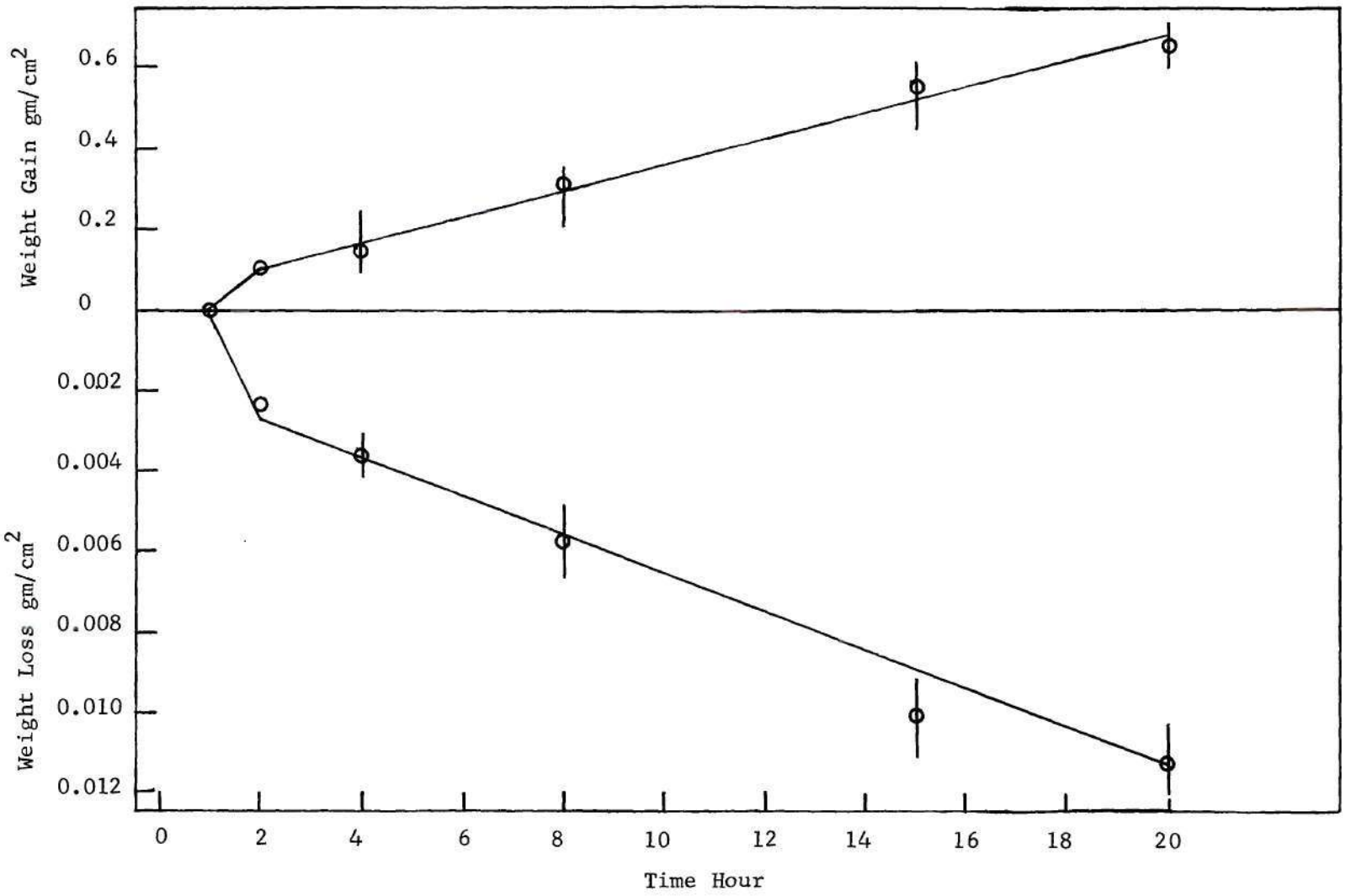

Figure 13. Weight Gain and Loss versus Time at 689°C.

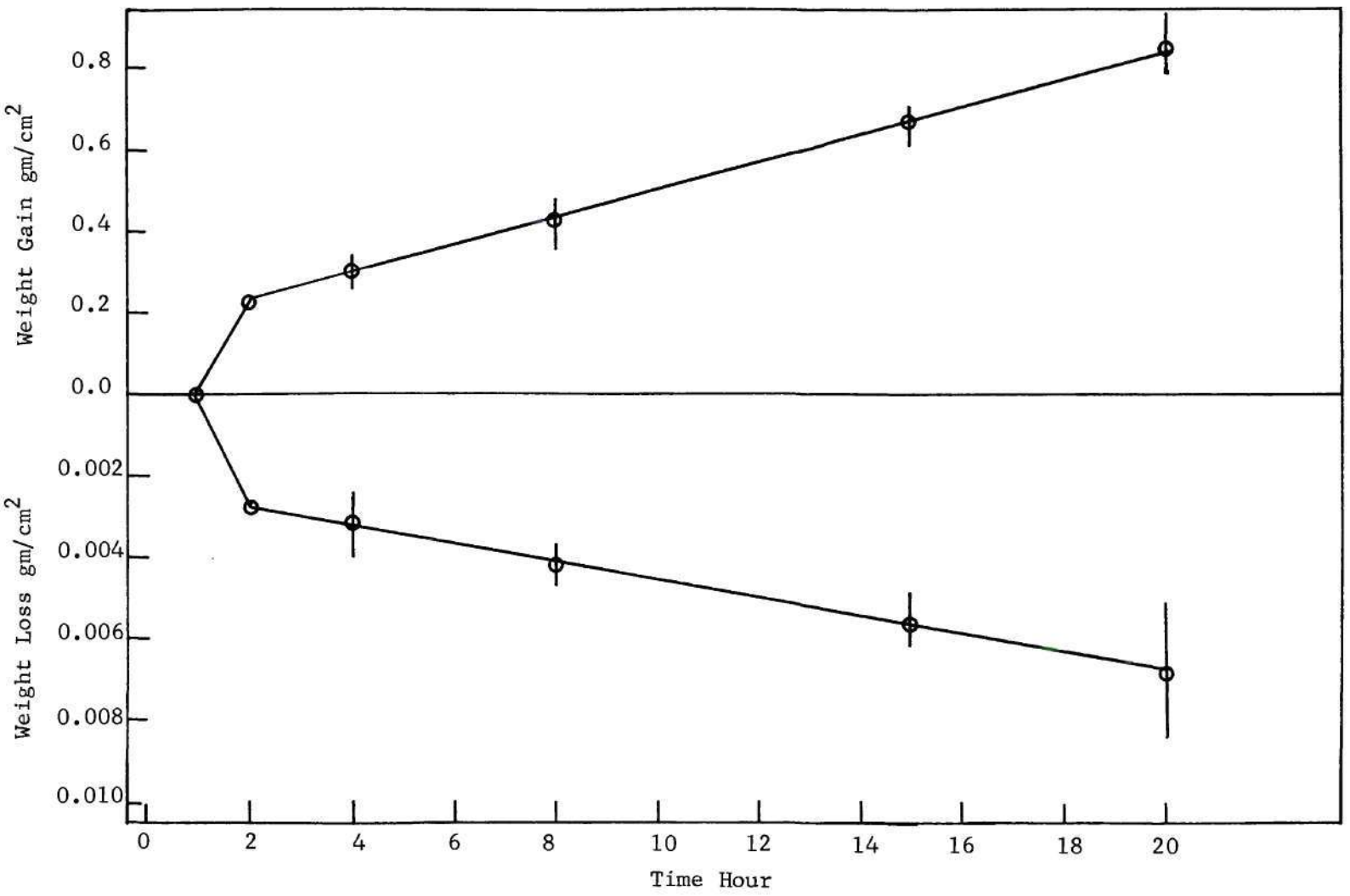

Figure 14. Weight Gain and Loss versus Time at 737°C.

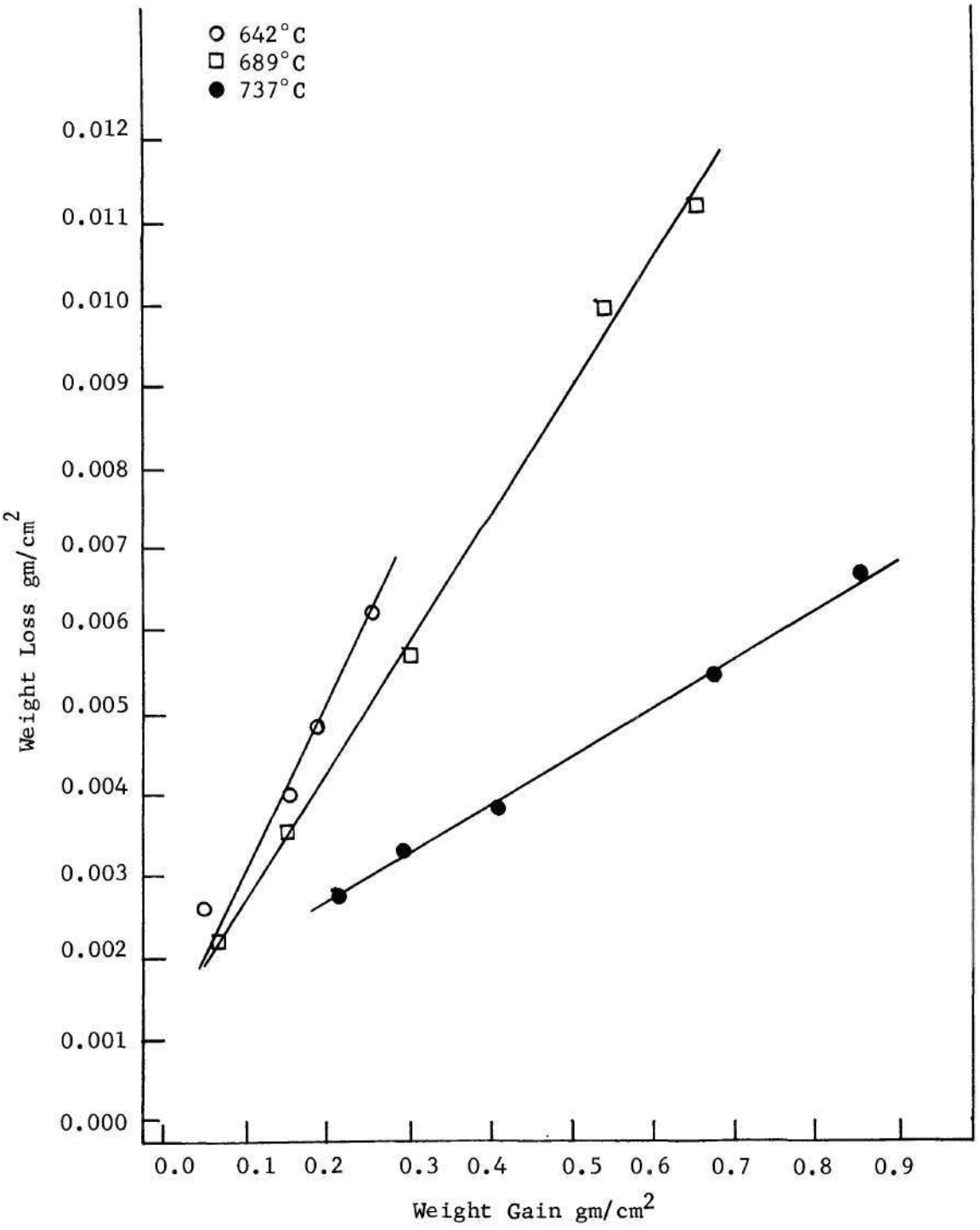

Figure 15. Weight Loss versus Weight Gain

Table 9. Reaction Rate Constant for Weight Gain and Loss

Temperature (°C)	Reaction Rate Constant (gm/cm^2 hr.) 642	689	737
Weight Gain	1.30×10^{-2}	3.27×10^{-2}	3.48×10^{-2}
Weight Loss	1.80×10^{-4}	4.90×10^{-4}	2.10×10^{-4}

of the wire. At 642°C great quantities of powdery carbonaceous dust formed around the wire. After 20 hours of reaction time, carbon deposits with a weight almost three times that of the wire had formed. The deposits formed completely surrounding the iron wire. Under the most severe reaction conditions enough carbon formed to plug the reaction tube. The amount of carbon formed increased with temperature until 735°C. At temperatures higher than this, the amount of carbon decreased. At 786°C the weight of carbon formed was less than one percent of the amount formed at the temperatures of maximum reaction. The weight loss of the iron wire was affected by temperature in the same manner, except the maximum in the weight loss occurred at a lower temperature, approximately 690°C. At higher temperatures the loss of weight decreased until 786°C where no measurable loss of weight occurred. Figure 16 is a plot of the weight of carbon deposited and the weight loss of the iron wire versus temperature at four and twenty hours.

A conditioning of the quartz reactor tube was found to occur. After a few runs a thin opaque carbonaceous film deposited on the quartz in the heated zone. A dilute hydrofluoric acid solution was used to clean the walls causing the film to peel away. Once a film completely

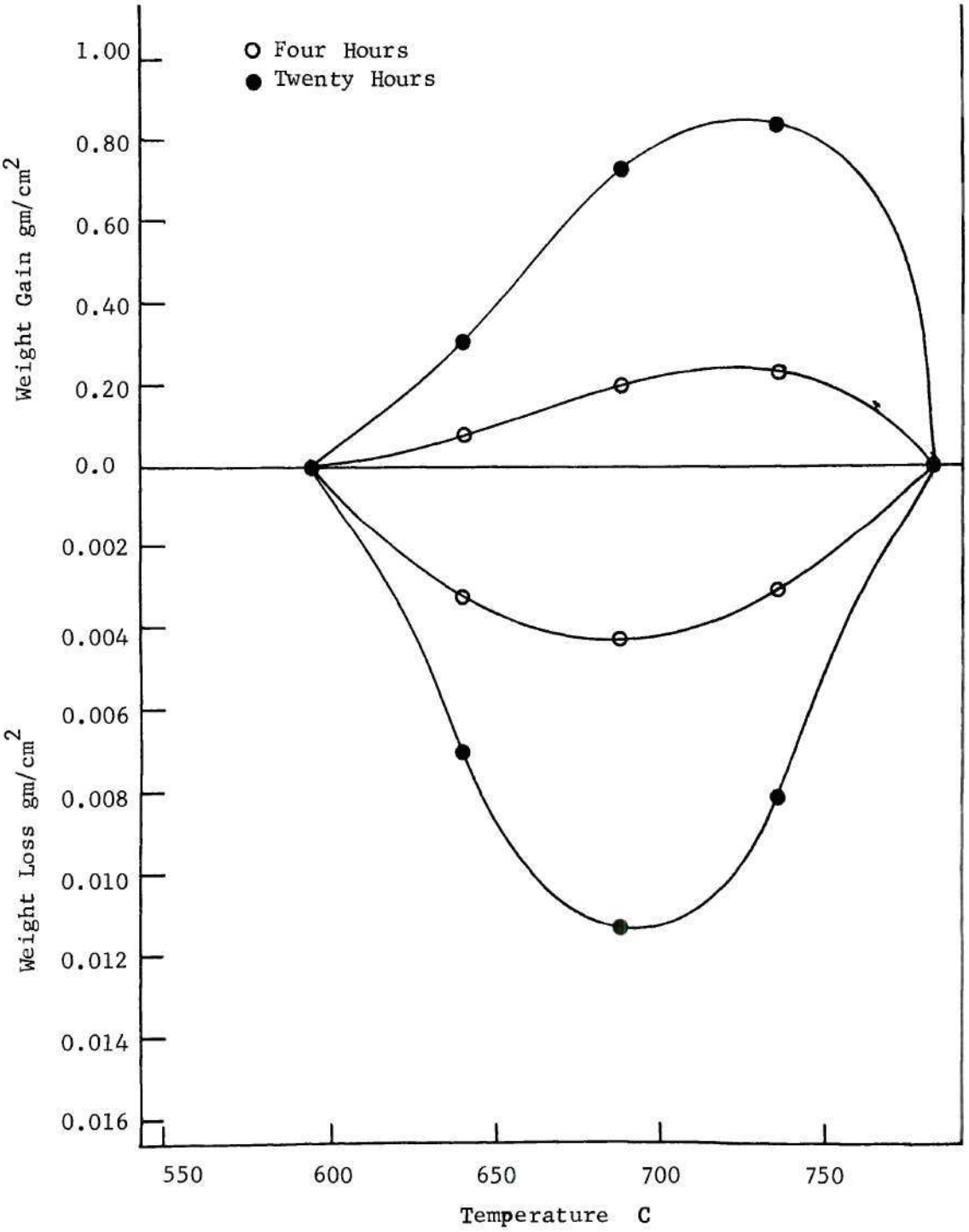

Figure 16. Weight Gain and Loss versus Temperature.

formed on the tube the build up stopped. After conditioning the only surface effect was due to the amount of iron surface exposed. At approximately 700°C the exit gas stream became foggy and condensation of some liquid products occurred outside the heated reaction zone. This condition increased with temperature.

The tube flow reactor was also packed with carbon and reacted with n-butane. There was no powdery carbon deposition on the packing during the n-butane pyrolysis.

Some samples were run for 120 hours to determine if the reaction would occur at a temperature below 595°C. Only a trace of weight gain and loss was observed at 548°C, and there was no evidence of a reaction at temperatures lower than 500°C.

Most of the experiments were done at a constant flow rate of 48.9 cc/min. A few runs were made varying the flow rates up to 87.0 cc/min. These results showed no significant difference from the constant flow results.

Polished cross sections of some representative samples of reacted wire were prepared to examine their structure. A nital acid etch was used. The surface of the wire was also examined in a scanning electron microscope. Figure 17 shows the cross section of a sample which had been reacted for twenty hours at 689°C. Some carburization of the sample has occurred. The interior of the cross section is composed of light colored ferrite with dark colored spheroidized cementite interdispersed among the ferrite. This structure is formed by carburization of the sample just below the euctectoid temperature and cooling slowly. Some of the cementite has formed along the grain boundaries. Some precipitation of cementite along the boundaries of the ferrite grains is expected

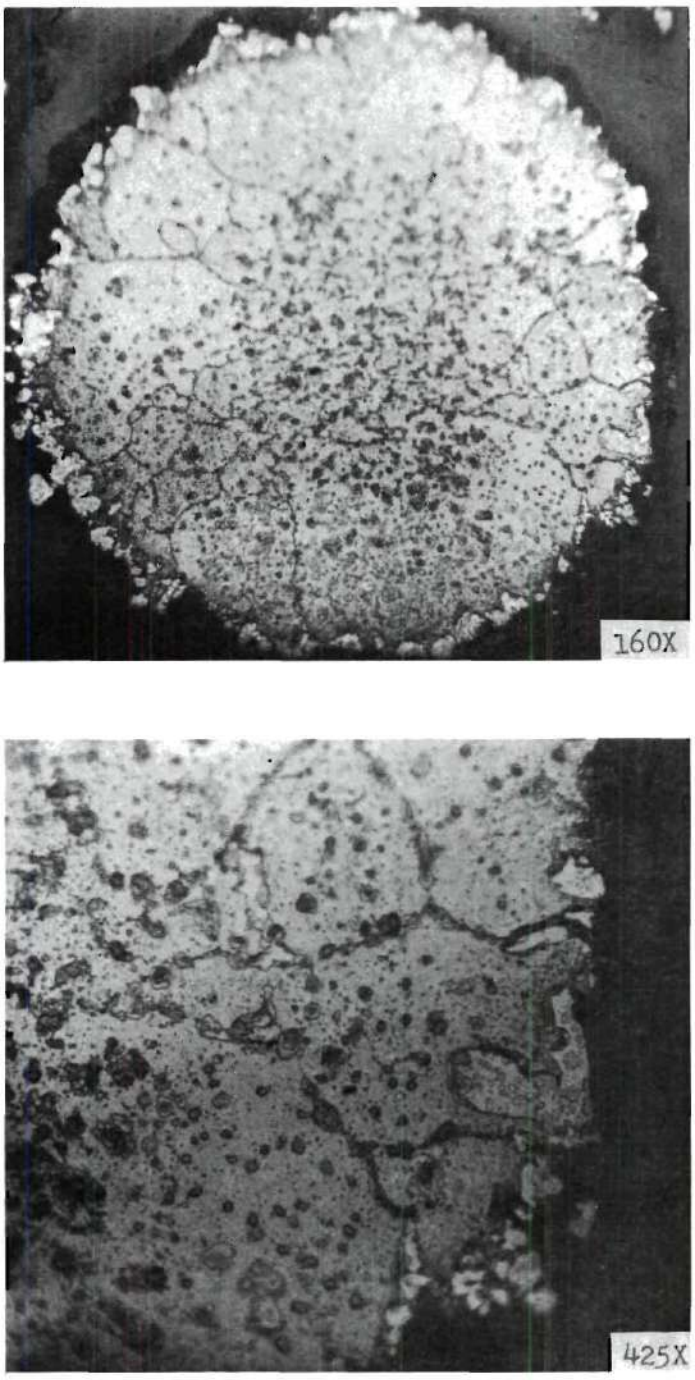

Figure 17. Cross Section of Sample Reacted at 689°C.

because of the decrease of the solubility of carbon in alpha iron upon cooling. At the edge of the cross section whole areas are detached from the light colored matrix into the dark boundary surrounding the cross section. This dark boundary is composed of cementite and perhaps some residual carbon deposits. Cementite was verified by etching some samples with alkaline sodium picrate which causes cementite to appear black.

Figure 18 shows the surface of this sample after the carbon deposits had been cleaned off. The surface is badly deteriorated and the diameter of the wire has been reduced from 0.020 inch to 0.018 inch. For comparison the surface of the wire before any reaction is also shown.

Figure 19 shows a metallographic cross section and a scanning microscopy photomicrograph of the surface of a sample reacted for twenty hours at 786°C. The dark areas in the interior are cementite and the light areas are ferrite. At this temperature, which is above the eutectoid, the solubility of carbon in iron is much greater (Figure 2) and the carburization of the sample is thus greater. However, the surface of the sample was not deteriorated. In fact, after the carbon deposit had been cleaned off, the surface as viewed by the SEM looked much the same as an unreacted surface.

The carbon deposits were in the form of a sooty powder that did not adhere readily to the surface. However, at 786°C where surface deterioration ceased, the deposit was a gray-silvery film much like the film formed on conditioning the quartz reactor. Figure 20 shows the deposits just beginning to form on the iron surface. The first deposits form at certain areas and then spread to cover the entire surface. Figure 21 shows

a.

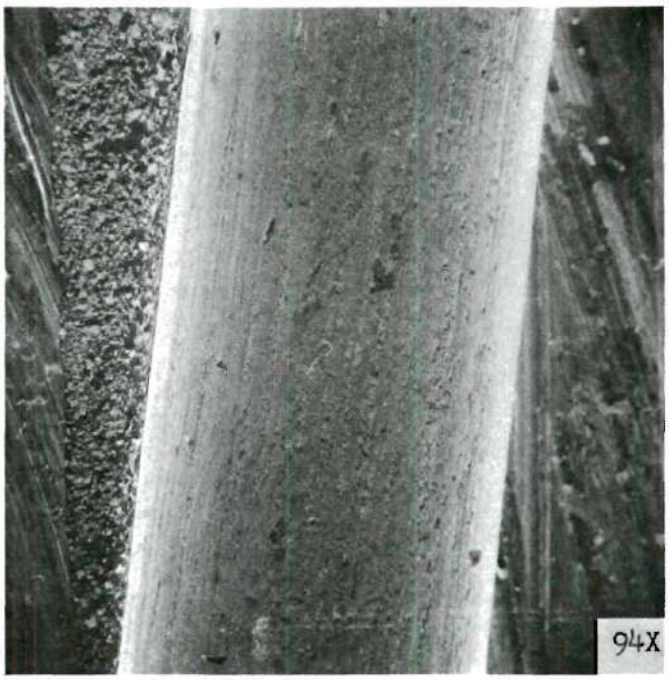

b.

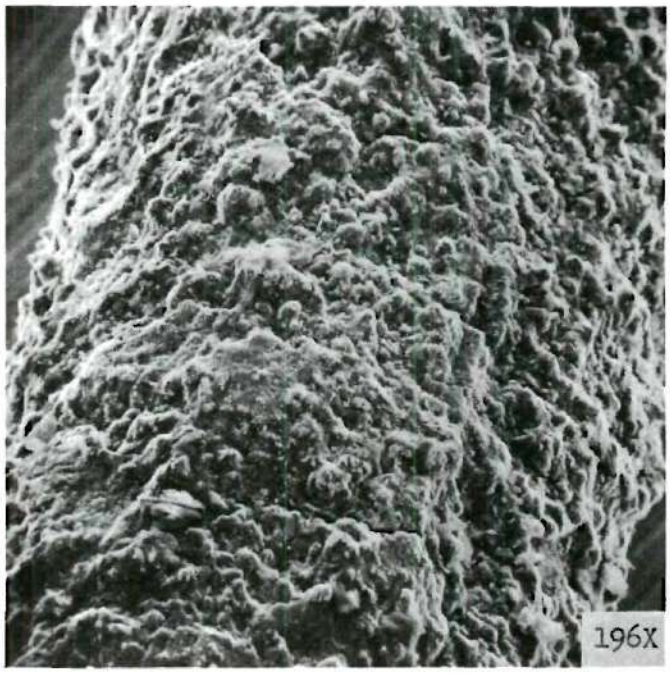

Figure 18. Surface of Iron Wire, a) Unreacted, b) Reacted at 689°C.

a.

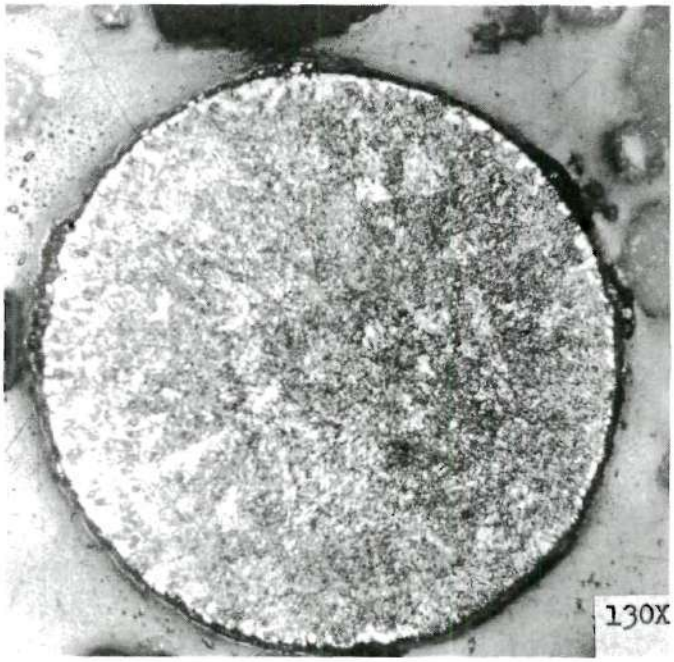

b.

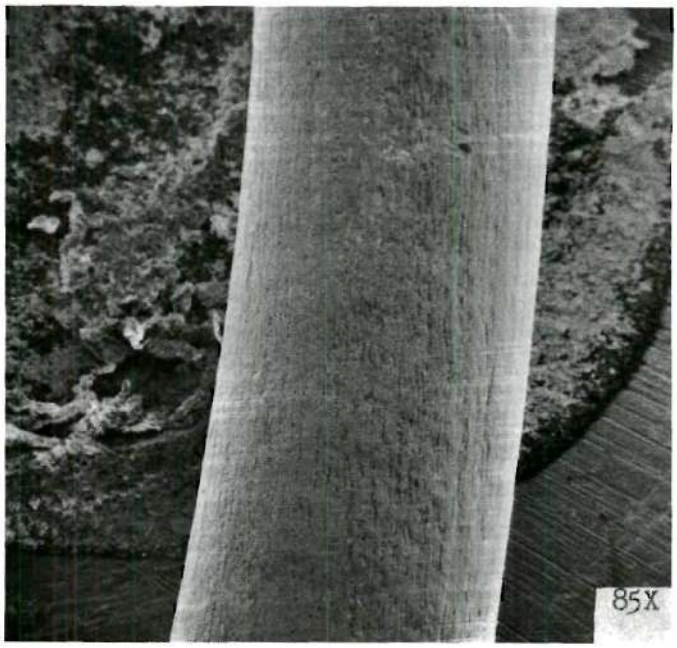

Figure 19. Cross Section and Surface of a Sample Reacted at 786°C, a) Cross Section, b) Surface.

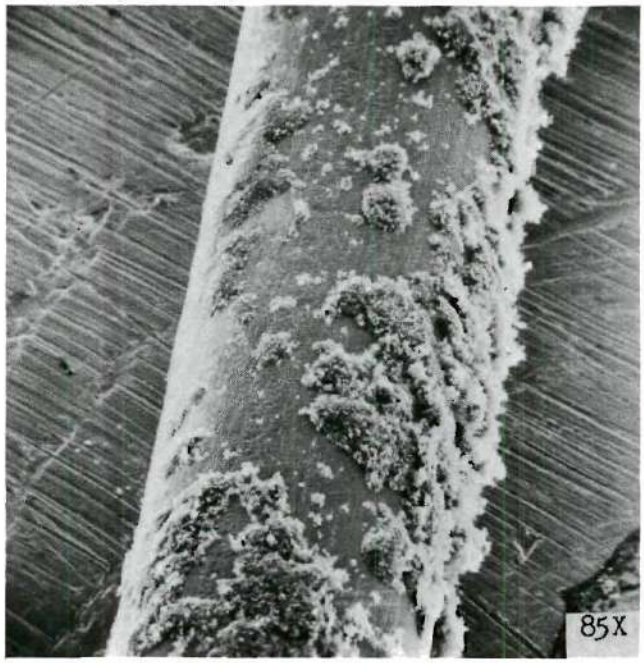

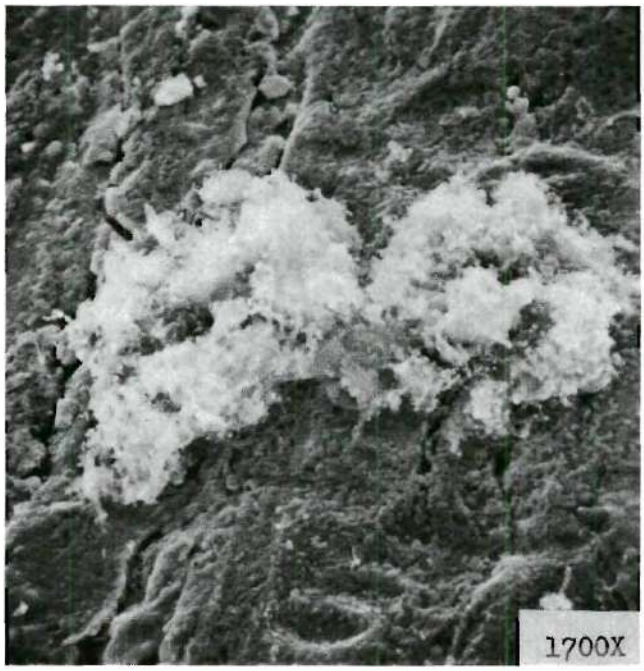

Figure 20. Initial Surface Deposits.

a.

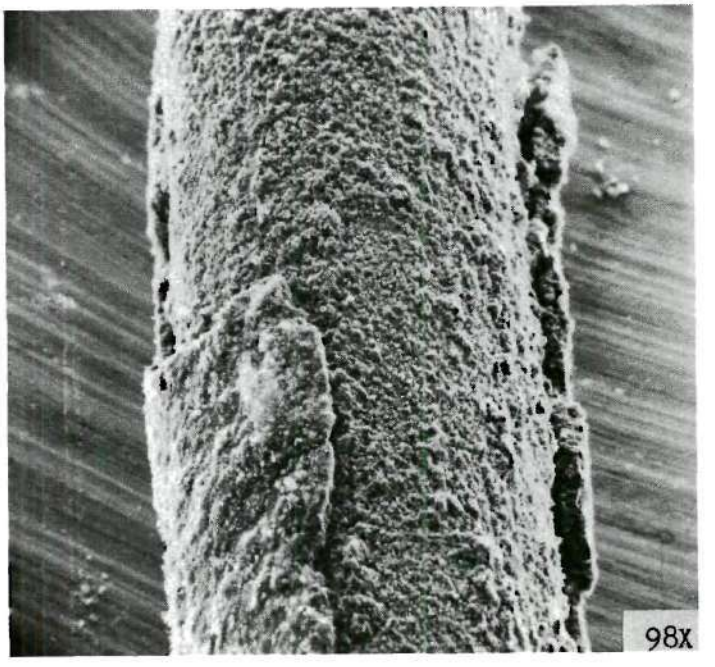

b.

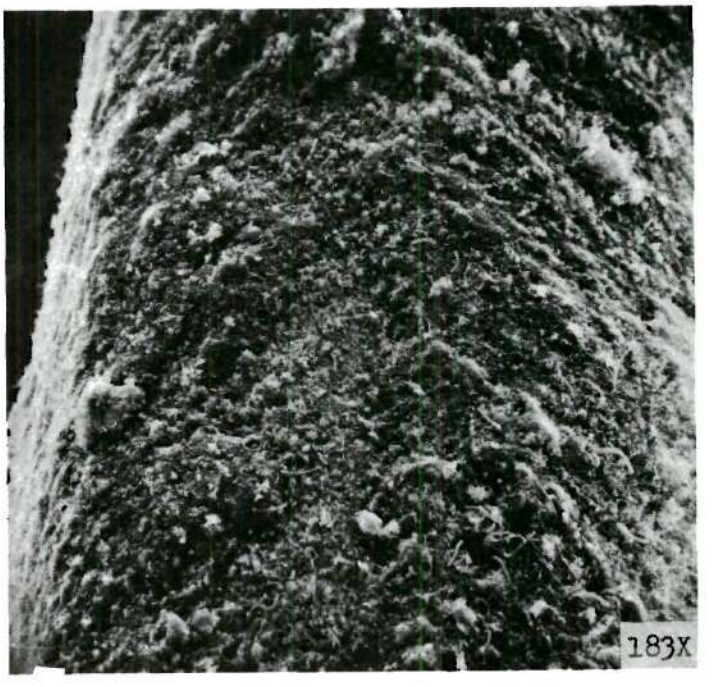

Figure 21. Surface Deposits After Twenty Hours of Reaction, a) 642°C, b) 737°C.

the carbon formed on the surface after twenty hours of reaction at 642°C and 737°C, respectively. Two different types of structure can be observed. The main deposit is a bulk type carbon and growing from the bulk deposits are filaments of carbon. The filamentary formation, although abundant, is considerably smaller in size and mass than the bulk formation. Figure 22 shows typical filamentary formation at 642°C and 737°C. As the temperature increased the length and diameter of the filaments also increased.

Discussion of Results

While hydrocarbons have been considered as contributing to the "metal dusting" reaction, methane has been shown experimentally to be relatively inert in a similar tubular flow reactor until well above the normal "metal dusting" temperatures (66, 68). However, a significant difference between methane and n-butane is the temperature range at which they decompose. It was calculated (see Appendix B) that for this tube flow reactor the temperature range for n-butane decomposition would be from 500° to 700°C while for methane it would be from 750° to 1050°C. In both cases decomposition of the hydrocarbon molecule occurs before carbon is deposited, but for n-butane this decomposition occurs at a much lower temperature.

Once n-butane begins to decompose, the gas reacts with the iron wire causing pitting and general deterioration of the iron surface and forming large amounts of carbon as a reaction product. The weight gain and loss curves versus time have the same general shape with both curves going through three stages: slow initial reaction, rapid reaction, and a steady rate of reaction. This is similar to reaction rate curves reported

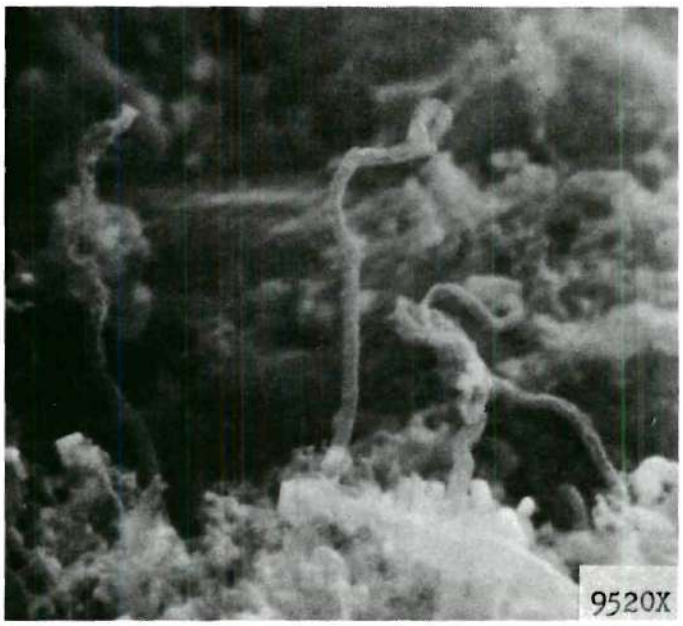

a.

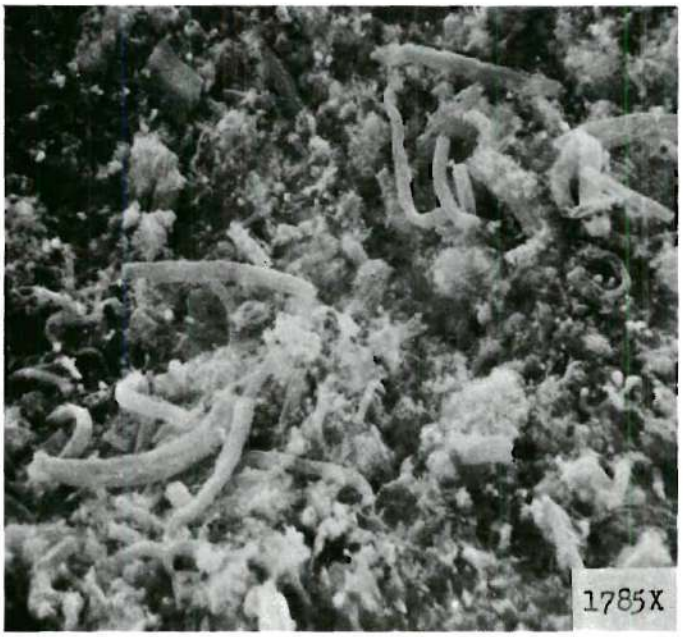

b.

Figure 22. Filamentary Formation of the Carbon Deposits, a) 642°C, b) 737°C.

by others (77, 79) for the carbon monoxide reaction with iron. The weight gain and loss at a particular temperature have a simple linear relation. This indicates that carbon formation and surface deterioration are both related and that one is in fact a measure of the other.

The reaction rate for carbon formation was more than 100 times greater with n-butane than with carbon monoxide. Several investigators (68, 77, 78) have found that small amounts of hydrogen or hydrogen-forming compounds drastically increase the rate of carbon formation with carbon monoxide. This hydrogen effect is thought to be related to the regeneration of iron from inactive iron carbide (77, 78, 97). A certain amount of hydrogen is formed during the n-butane pyrolysis. The extremely high rate of carbon formation with n-butane suggests that a hydrogen effect is occurring with this reaction.

Carbides can be formed on iron surfaces from carbon monoxide and hydrocarbons at the temperatures of this reaction (98). Metallographic studies showed a layer of cementite on the outer surface of the wire samples reacted in this experiment. Haas et al. (77) have shown that with carbon monoxide a carbide layer was formed very quickly on iron catalysts. The density of cementite is reported to be 7.70 gm/cm^3 (98) as compared with 7.87 gm/cm^3 (99) for pure iron. Thus the molar volume of cementite is larger than the original iron material and it would form a compact product layer on the catalyst surface. The stability of the carbide layer and diffusion of iron through the layer are considered limiting factors in the reaction of carbon monoxide with iron. However, the n-butane pyrolysis can produce free hydrogen which will regenerate the carbide to iron. Thus the carbide layer, while an important step of

the overall reaction, would not limit this reaction nearly as much as in the case of carbon monoxide.

The sooty carbon surface deposits first build up on the wire at certain areas and then spread over the entire surface. The carbon appears on the surface in two forms: (1) a filamentary type of growth and (2) a bulk type carbon. The average diameter and length of the filaments increased with temperature. These two forms of carbon have been reported by several other workers (84, 85, 86) investigating carbon formation on iron surfaces. Several people (66, 81, 82) also found evidence of iron or carbides of iron migrating with the filaments.

The process that starts with pyrolysis of small hydrocarbons and ends with large carbon particles must involve not only decomposition but also growth of particles as well as dehydrogenation. The low pressure study of the pyrolysis of n-butane over iron showed that the iron not only catalyzed the pyrolysis but influenced the hydrogen content of the products. The products, mainly C_2 hydrocarbons, are well suited for polymerization reactions. While observation of fogs or mists in the tubular flow reactor indicates a certain amount of polymerization, no carbon is formed without iron wire in the reaction chamber. The iron must be present to provide active catalytic sites for carbon build-up. At each temperature the amount of carbon formed is proportional to the weight loss of iron suggesting that the process of carbon formation and metal loss are directly related.

There is a great difference between the type of carbon formed on the wire sample at 786°C and at lower temperatures. At 786°C, instead of great quantities of sooty non-adherent deposits, a grey-silvery deposit

forms which covers the entire surface. The weight of this carbon deposit is only a fraction of the weight of the sooty deposits. While the wire sample itself is carburized, the surface does not deteriorate. Almost certainly the main factor influencing this change is the eutectoid transformation of iron-iron carbide at 723°C. Below 723°C iron is in the body centered cubic phase ferrite. Above 723°C, the face centered cubic (austenite) phase can be formed. Between 723° and 910°C and at appropriate carbon concentrations, a two phase mixture of austenite and ferrite exists (Figure 2). An important feature of austenite compared to ferrite is its ability of dissolve carbon. The maximum solubility of carbon in ferrite is 0.0025 weight percent carbon at 723°C while austenite can dissolve 0.8 weight percent at 723°C with the solubility increasing with temperature to nearly 2.0 weight percent at 910°C. Below the eutectoid temperature the solubility of carbon in iron is small and after saturation excess carbon can only be accommodated in iron by carbide formation. However, above the eutectoid temperature a state of equilibrium is set up between the ferrite and austenite phases. Once austenite begins to form absorption of carbon at the surface will take place only via the austenitic phase until saturation and then progressive transformation of ferrite to austenite proceeds as carbon continues to be absorbed. This will lead to a growth of austenite from the surface to the interior.

Westerman (79) also observed the same change in the type of carbon deposited from carbon monoxide when the reaction temperature passed the eutectoid point. In this experiment with n-butane there was still sooty carbon formation up to 737°C, although the amount of surface deterioration

had begun to fall off. However, the n-butane pyrolysis is endothermic (18) and one can expect significant temperature gradients between the pyrolyzing gas and the surface on which carbon is deposited. Some of the wire surface could still be below the eutectoid and susceptible to sooty carbon formation. The fall off in surface deterioration would be due to a reduction in the available catalytic sites. The amount of carbon formation depends not only on these sites but also on aggregation and growth of carbon. If the aggregation and growth process increases enough, then carbon formation will still increase while metal loss decreases. Once the wire is above the eutectoid the grey-silvery deposit forms and surface deterioration ceases. At this point the reaction is just one of diffusion controlled carburization.

A change in gas flow from 49 to 87 cc/min had little or no effect on carbon deposition or metal loss. Therefore bulk gas diffusion to the surface does not appear to be a factor. The equilibrium composition of the gas was primarily carbon and hydrogen. The reaction therefore was not limited by thermodynamic considerations.

Discussion of Mechanism

It is recognized that the actual mechanism of this complex reaction cannot be easily ascertained from the available kinetic data. However, this data will assist in establishing the rate controlling parameters.

The presence of iron wire during the pyrolysis of n-butane has been shown to catalyze the decomposition of the gas and to act as a site for carbon formation. Carbon formation, moreover, is accompanied by a general deterioration and pitting of the wire surface.

The increase in the rate of decomposition of n-butane is

proportional to the catalyst surface available. This is indicative of a reaction on the surface of the catalyst. This surface reaction of the iron can be thought of as proceeding in the following stages:

1. Reactants diffuse from a homogenous gas phase to the catalyst surface.
2. Reactants are adsorbed on the catalyst surface.
3. Chemical reaction takes place at the surface.
4. Product gas molecules are desorbed from the catalyst surface.
5. Desorbed gas product molecules diffuse away from the catalyst surface.

Gas diffusion to and from the catalyst surface does not appear to be a major factor since the changes in gas flow had little or no effect on the rate. Physical adsorption processes exhibit a low activation energy, whereas chemisorption and chemical reactions occur with rather high activation energies. The activation energies in the constant rate period for both carbon formation and metal loss are more in line with what is expected from chemisorption and chemical reaction rather than physical adsorption.

The precise path of the chemical reaction is quite complex involving carbon formation, carbide formation, carbide decomposition and iron regeneration from the available hydrogen. These reactions result in a deterioration of the surface accompanied by a great amount of carbon formation with iron or carbide being transported from the surface with the carbon deposit.

Carbon formation does not occur without iron as a catalyst. The amount of carbon formed depends not only on the active catalytic sites

but also on aggregation and growth of carbon. Carbon can be formed either directly by a polymerization and dehydrogenation of a sorbed molecule or indirectly by the decomposition of cementite which forms on the iron surface. The decomposition of cementite to graphite and iron is the mechanism of carbon formation during the reaction of carbon monoxide and iron. The amount of carbon formed, however, is much less than for the n-butane reaction. Unlike the carbon monoxide reaction, conditions favor the direct formation of carbon during the n-butane pyrolysis. The initial products of the n-butane decomposition on iron, mainly C_2 hydrocarbons, are well suited for polymerization and iron is known to be an active dehydrogenation catalyst (7, 100). Since much more carbon is available, more carbon should be formed by this mechanism than the indirect mechanism. For the n-butane reaction it is likely that carbon is mostly formed directly by the polymerization and dehydrogenation of sorbed species.

Carbon formation is accompanied by a general surface deterioration. Filamentary carbon growth proceeds with iron being removed from the surface of the metal into the filament (66, 81, 82). However, filamentary carbon make up only a fraction of the carbon deposited and it does not seem likely that this could account for all of the surface deterioration.

Surface deterioration can also occur by heavy intergranular attack of the metal and grain removal by carbon deposits at the grain boundary (66). The action of hydrogen, available from the n-butane pyrolysis, can regenerate iron from cementite exposing more area to attack (77, 78, 97). Figure 17 and 18 showing intergranular attack and pitting of a reacted sample, indicate that surface deterioration is also occurring by this mechanism.

Carbon formation with its accompanied surface deterioration did not occur, at least to any measurable extent, at temperatures below 500°C, the lower range of homogenous decomposition of n-butane for this tubular flow reactor. Decomposition of the gas must first occur for carbon to form directly by polymerization and dehydrogenation. Also below 500°C indirect carbon formation through cementite decomposition does not occur (79). Above the eutectoid temperature the type of carbon formed changes from loosely adherent powdery dust to a grey silvery adherent film. The amount of carbon deposited is very much less and surface deterioration stops. At these temperatures, "metal dusting" ceases and carburization begins.

Comparison of n-Butane and Carbon Monoxide "Metal Dusting

The most striking difference between the two "metal dusting" reactions with iron is the two order of magnitude increase in the rate of carbon formation with n-butane. Carbon monoxide will not decompose at these temperatures without the aid of a catalyst. Therefore carbon is formed by a mechanism of adsorption and decomposition of an intermediary carbide in the case of iron catalysts. However, n-butane does decompose homogeneously at these temperatures, but iron is necessary to catalyze carbon formation. Carbon can form on iron not only indirectly through cementite decomposition but also directly through polymerization and dehydrogenation. Furthermore hydrogen can act to regenerate iron from carbide.

The rate of carbon formation versus time or temperature are qualitatively very much the same for both reactions. This type of rate curve is characteristic of many reactions which are catalyzed by solid surfaces. The maximum carbon formation occurs at different temperatures for the

two reactions, due likely to the different mechanisms for carbon formation encountered and the decomposition characteristics of the gas.

The surface reactions seem quite similar with n-butane and carbon monoxide. In both cases surface deterioration occurs through migration of metal from the surface into the filamentary carbon growth and by intergranular attack of the metal and grain removal by carbon deposits. However, since metal loss is proportional to the amount of carbon formed the deterioration is much more severe with n-butane than with carbon monoxide.

"Metal dusting" stops above the eutectoid temperature in both reactions and normal carburization occurs. However, carbon monoxide "metal dusting" does not occur to an appreciable extent below 450°C and n-butane "metal dusting" does not occur until temperatures above 500°C and decomposition of the hydrocarbon begins.

CHAPTER V

CONCLUSIONS

1. Bulk iron catalyzes the decomposition of n-butane by a surface reaction. The initial reaction products are mainly the C_2 hydrocarbons ethane, ethylene and acetylene.

2. The reaction of pure alpha iron with pure n-butane above its decomposition temperature results in carbon formation on the iron surface. The carbon formation is accompanied by a general deterioration and pitting of the iron surface. Carbon formation does not occur without iron to act as a catalyst.

3. At each temperature the weight of carbon formation is proportional to the loss of weight of the iron surface.

4. Carbon forms for the most part directly from the polymerization and dehydrogenation of sorbed species. Metal loss occurs through the migration of iron from the surface into the filamentary carbon growth and by intergranular attack of the metal and grain removal by carbon deposits at the grain boundary.

5. The carbon formed consists of: (1) filamentary growth, and (2) flake or bulk deposits. The length and diameter of the filaments increase with temperature.

6. Above the eutectoid temperature surface deterioration stops and only a small amount of carbon is deposited. Carburization of the iron is then the principle reaction.

7. n-Butane "metal dusting" on iron is much more severe than

carbon monoxide attack. More than 100 times the amount of carbon is formed during n-butane attack promoting more severe surface deterioration.

CHAPTER VI

RECOMMENDATIONS

This research established that hydrocarbons do cause "metal dusting", that carbon formation and surface deterioration are directly related and proceed through a surface reaction, and that "metal dusting" with n-butane is much more severe an attack than with carbon monoxide. While a general outline of the surface reaction was established, an extension of this work to study the exact mechanism of carbon formation and metal deterioration would be helpful. For both carbon monoxide and n-butane "metal dusting" stopped for iron at the eutectoid. The reason for this is not altogether clear and needs investigation. The susceptibility of iron alloys, especially the stainless steels, needs to be determined for hydrocarbon "metal dusting" since industrial problems seem to occur most frequently with stainless steels.

An interesting study would be the reaction of isobutane over iron. Isobutane, while decomposing in approximately the same temperature range as n-butane, forms a completely different product spectrum. A study of this system should give some idea as to the importance of the decomposition products in carbon formation. Of course the ultimate goal is not just to describe the reaction but to control or prevent carbon formation and metal deterioration. Gas phase inhibitors that poison the reaction sites or deactivate the surface seem to be the most likely solution. It is recommended that work also be carried out in this area.

APPENDICES

APPENDIX A

FLOW KINETICS AND CALCULATION OF K_e FOR LOW PRESSURE PYROLYSIS

The mechanism can be represented by the following set of kinetic equations in which A represents a reactant molecule (89).

$$\begin{array}{l} A \xrightarrow{K} \text{products} \\ \quad\ \ \xrightarrow{K_e} \text{escape through aperture} \end{array}$$

If:

N_A = steady state flow rate of A into the reactor (moles/sec)

C_A = steady state concentration of A in the reactor (moles/liter)

V = reactor volume (liters)

K = first order rate constant for A

K_e = first order escape rate constant for A

Then at steady state:

$$N_A - KC_AV - K_eC_AV = 0$$

$$C_A = \frac{N_A}{(K_e + K)V}$$

The mass spectrometer signal for A is proportional to the flux of A escaping from the reactor.

$$I_A = \alpha_A K_e C_A V = \alpha_A \frac{K_e N_A}{K_e + K}$$

Where: I_A = mass spectrometer signal from A

α_A = constant of proportionality between the signal and flux of A.

At low temperatures where no reaction takes place we observe a signal:

$$I_A^\circ = \alpha_A N_A$$

Dividing I_A by I_A° and solving for K gives:

$$\frac{I_A}{I_A^\circ} = \frac{K_e}{K + K_e}$$

$$K = K_e \frac{(I_A^\circ - I_A)}{I_A}$$

Calculation of K_e

From kinetic theory Dushman (101) shows that the conductance of a tube at very low pressure is:

$$F = 11.428\ a^2 K\sqrt{T/M}\ \text{liter sec}^{-1}$$

where:

F = conductance (liter/sec)

a = radius of tube (cm)

K = Clausing's factor

T = absolute temperature ($^\circ$K)

M = molecular mass (gm)

K_e, the first order escape rate constant for butane, is simply the possible conductance of butane from the reactor divided by the volume of the reactor.

$$K_e = F/V = 11.428\ a^2 K\sqrt{T/M}\ /V\ \text{sec}^{-1}$$

For this reactor:

a = 0.41 cm

l = 3.81 cm

l/a = 9.20

From Dushman (100) K = 0.215

V = 0.125

M = 58.12 gm

$K_e = 0.442\ T^{\frac{1}{2}}\ \text{sec}^{-1}$

APPENDIX B

CALCULATION OF THE TEMPERATURE RANGE FOR THE DECOMPOSITION OF n-BUTANE AND METHANE IN THE TUBE FLOW REACTOR

Assuming irreversible first order reaction and plug flow, a balance on an incremental volume for reactant A gives:

$$N_A - (N_A + dN_A) - K\, C_A dV_R = 0 \qquad (1)$$

where:

N_A = reactant molar feed rate (#moles/sec)

V_R = reactor volume (ft^3)

K = rate constant (sec^{-1})

C_A = reactant concentration (#moles/ft^3)

letting:

X_A = fractional conversion

δ_A = fractional change in the volume between no and complete conversion

then:

$$N_A = N_A^\circ\ (1 - X_A)$$

$$C_A = N_A/V_A = N_A^\circ\ (1 - X_A)/V_o\ (1 + \delta_A X_A)$$

V_o = volumetric flow rate

Substituting into (1) gives:

$$\int_o^{X_A} \frac{1 - X_A}{1 + \delta_A X_A}\, dX_A = \frac{K}{V_o} \int_o^{V_R} dV_R$$

$$K \frac{V_R}{V_o} = - (1 + \delta_A) \ln (1 - X_A) - \delta_A X_A$$

For this particular reactor:

$$V_R = 4.48 \times 10^{-3} \text{ ft}^3$$

$$V_o = 2.88 \times 11^{-5} \text{ ft}^3/\text{sec}$$

Thus:

$$155.55 K = - (1 + \delta_A) \ln (1 - X_A) - \delta_A X_A$$

For n-Butane:

$$\delta_A = 1$$

$$\log_{10} K = 12.71 - 58{,}700/2.303RT \quad (3)$$

$$155.55K = - 2 \ln (1 - X_A) - X_A$$

at $500^\circ C$ $X_A = .026$

$650^\circ C$ $X_A = .999$

For Methane:

$$\delta_A = 0$$

$$\log_{10} K = 15.3 - 104{,}000/2.303RT \quad (14)$$

$$155.55K = - \ln (1 - X_A)$$

at $800^\circ C$ $X_A = .001$

$1050^\circ C$ $X_A = .903$

BIBLIOGRAPHY

1. R. N. Pease, "The Thermal Dissociation of Ethane, Propane, n-Butane and i-Butane," Journal of the American Chemical Society, 50, 1779 (1928).

2. R. N. Pease and E. S. Durgan, "The Kinetics of the Thermal Dissociation of Propane and the Butanes," Journal of the American Chemical Society 52, 1262 (1930).

3. E. W. R. Steacie and I. E. Puddington, "The Kinetics of the Decomposition Reactions of the Lower Parraffins. I. n-Butane," Canadian Journal of Research Section B16, 176 (1938).

4. P. D. Pacey and J. Howard Purnell, "Propylene from Parrafin Pyrolysis," Industrial and Engineering Chemistry Fundamentals 11, 233 (1972).

5. S. L. K. Wittig, "Study of the Thermal Decomposition of n-Butane," The Physics of Fluids Supplement I, I-133 (1969).

6. F. O. Rice and K. F. Herzfeld, "The Mechanism of Some Chain Reactions," Journal of Physics and Colloidal Chemistry 55, 975 (1951).

7. S. W. Benson, The Foundations of Chemical Kinetics, McGraw-Hill Book Company, Inc., New York (1960).

8. F. O. Rice, W. R. Johnson, and B. L. Evering, "The Thermal Decomposition of Organic Compounds from the Standpoint of Free Radicals," Journal of the American Chemical Society 54, 3529 (1932).

9. F. O. Rice and K. K. Rice, The Aliphatic Free Radicals, John Hopkins, Baltimore (1935).

10. L. S. Echols and R. N. Pease, "Kinetics of the Decomposition of n-Butane," Journal of the American Chemical Society 61, 208 (1939).

11. J. H. Purnell and C. P. Quinn, "The Pyrolysis of n-Butane," Proceedings of the Royal Society London, Series A, 270, 267 (1962).

12. N. H. Sagert and K. J. Laidler, "Kinetics and Mechanism of the Pyrolysis of n-Butane," Canadian Journal of Chemistry 41, 838 (1963).

13. C. H. Bamford and C. F. H. Tipper, Comprehensive Chemical Kinetics Vol. 5, Elsevier Publishing Company, Amsterdam (1972).

14. S. W. Benson, "Kinetic Data on Gas Phase Unimolecular Reactions," A.S.R.D.S. No. 21, 1970.

15. A. Torbk, The Kinetics of the Pyrolysis of n-Butane, Ph.D. Thesis, University of Toronto (1969).

16. S. Sandler and Y. Chung, "High Temperature Pyrolysis of n-Butane," Industrial and Engineering Chemistry 53, 391 (1961).

17. P. Poyhonen and V. Veijola, "Thermal Decomposition of n-Butane in a Flow Reactor," Kem. Teollisuus 4, 27 (1970).

18. P. H. Calderbank, "Some Problems in the Design of Light-Hydrocarbon Pyrolysis Coils," Chemical Engineering Progress 50, Symposium Service No. 9, 53 (1954).

19. J. H. Purnell and C. P. Quinn, "The Role of Surfaces in the Pyrolysis of n-Butane," Journal of the Chemical Society 4138 (1961).

20. H. Eyring, Annual Review of Physical Chemistry 21, Annual Reviews, Inc., Palo Alto, California, 197 (1970).

21. R. O. King, S. Sandler, and Y. H. Chung, "The Production of Ethylene by the Decomposition of n-Butane; The Prevention of Carbon Formation by the Use of Chromium Plating," Transactions of the Engineering Institute of Canada 3, 1 (1959).

22. P. P. Smith, "Equilibrium of Iron-Carbon Alloys with Mixtures of CO-CO_2 and CH_4-H_2," Journal of the American Chemical Society 68, 1163 (1946).

23. Max Hansen, Constitution of Binary Alloys 2nd Edition, McGraw-Hill Book Co., Inc., New York (1958).

24. Metal Progress Data Sheet No. 32 (1946).

25. R. A. Buckley and W. Hume-Rothery, "Liquidus and Solidus Relations in Iron-rich Iron-Carbon Alloys," Journal of the Iron and Steel Institute 196, 403 (1960).

26. Samuel Epstein, The Alloys of Iron and Carbon Vol. I, McGraw-Hill Book Co., Inc., New York (1936).

27. Y. Lakhtin, Engineering Physical Metallurgy, Gordon and Breach, Science Publishers, Inc., New York (1965).

28. R. W. Cahn, Physical Metallurgy, American Elsevier Publishing Company, Inc., New York (1970).

29. Robert M. Brick, Robert B. Gordon, and Arthur Phillips, Structure and Properties of Alloys, McGraw-Hill Book Co., Inc., New York (1965).

30. R. Mehl and C. Wells, "Constitution of High-purity Iron-Carbon Alloys," Transactions AIME 125, 429 (1937).

31. C. Wells, "Graphitization in High Purity Iron-Carbon Alloys," Transactions: American Society for Metals 26, 289 (1938).

32. R. Gurry, "The Solubility of Carbon as Graphite in Gamma Iron," Transactions AIME 150, 147 (1942).

33. L. Darken and R. Gury, "Free Energy of Formation of Cementite and the Solubility of Cementite in Austenite," Transactions AIME 191, 1018 (1951).

34. P. Pingualt, "Formation and Decomposition of Cementite," Academie des sciences, Paris. Comptes rendus hebdomadaires des seances 191, 1007 (1930).

35. S. B. Hendricks, "Crystal Structure of Cementite," Zeitschrift Kristallographic 74, 534 (1930).

36. L. J. E. Hofer, E. M. Cohn, and W. C. Peebles, "The Modifications of the Carbide, Fe_2C; Their Properties and Identifications," Journal of the American Chemical Society 71, 189 (1949).

37. G. Hagg, "Powder Photographs of a New Iron Carbide," Zeitschrift Kristallographic 89, 92 (1934).

38. K. H. Jack and S. Wild, "Nature of the x-carbide and its Possible Occurrence in Steels," Nature 212, 248 (1966).

39. J. P. Senateur, "Magnetic and Structural Study of the Hagg Carbide," Annales de Chimie (Pares) 14, 103 (1967).

40. H. Schenk et al., Forschungsber. Landes Nordrein-Westfalen, No. 1589, p. 81 (1966).

41. E. M. Cohn and L. J. E. Hofer, "Some Thermal Reactions of the Higher Iron Carbides," Journal of Chemistry and Physics 21, 354 (1953).

42. L. J. E. Hofer and E. M. Cohn, "Saturation Magnetizations of Iron Carbides," Journal of the American Chemical Society 81, 1576 (1959).

43. L. J. E. Hofer, "Nature of the Carbides of Iron," H. S. Bureau of Mines Bulletin 631, (1966).

44. M. Okada and Y. Arata, "X-Phase (Fe_2C) in Tempering Carbon Steels," Journal of the Japan Institute of Metals 19, 186 (1955).

45. S. Nagakuro, "Study of Metallic Carbides by Electron Diffraction," Journal of the Physical Society of Japan 14, 186 (1959).

46. H. C. Eckstrom and W. A. Odcock, "A New Iron Carbide in the Hydrocarbon Synthesis Catalyst," Journal of the American Chemical Society 72, 1042 (1950).

47. F. H. Herbstein and J. A. Snyman, "Identification of Eckstron-Adcock Iron Carbide as Fe_7C_3," Inorganic Chemistry 3, 894 (1964).

48. Y. Tamai and Y. Nishiyama, "Surface Effects on the Thermal Decomposition of Hydrocarbons," Bulletin of the Japan Petroleum Institute 12, 16 (1970).

49. B. L. Crynes and L. F. Albright, "Pyrolysis of Propane in Tubular Flow Reactors," I. and E. C. Process Design and Development 8, 25 (1969).

50. Y. Nishiyama, "Effect of Metallic Surfaces on the Thermal Decomposition of Ethane," Bulletin of the Chemical Society of Japan 42, 2494 (1969).

51. H. B. Palmer and C. F. Cullis, "The Formation of Carbon From Gases," Chemistry and Physics of Carbon 1, 265 (1965).

52. R. O. Grisdale, A. C. Pfister, and W. van Roosbroeck, "Pyrolytic Film Resistors: Carbon and Borocarbon," The Bell System Technical Journal 30, 271 (1951).

53. H. R. Grane, J. E. Connor, and G. P. Masologites, "The Behavior of Metal Contaminants in Catalytic Cracking," API Division of Refining 41 III, 241 (1961).

54. Y. Tamai, Y. Nishiyama and M. Takahashi, "Carbon Deposition on Iron and Nickel Sheets from Light Hydrocarbons," Carbon 6, 593 (1968).

55. Y. Tamai, Y. Nishiyama and M. Takahashi, "The Effects of Hydrogen and Helium Upon Carbon Deposition Onto Metal Surfaces," Carbon 1, 209 (1969).

56. S. D. Robertson, "Carbon Formation from Methane Pyrolysis over Some Transition Metal Surfaces - I. Nature and Properties of the Carbons Formed," Carbon 8, 365 (1970).

57. R. O. King, S. Sandler, and Y. H. Chung, "The Production of Ethylene by the Decomposition of n-Butane; The Prevention of Carbon Formation by the Use of Chromium Plating," Transaction of the Industrial and Engineering Chemistry 3, 1 (1959).

58. A. I. KuKina, V. B. Evdokimov and L. I. Barsova, "Catalytic Transformation of Butane on -Fe and Its Oxides," Kinetikai Kataliz, Akad. Navk SSSR, Sb. Statei 204 (1960).

59. E. Camp, C. Phillips and L. Gross, "Corrosion of 18-8 Alloy Furnace Tubes in High Temperature Vapor Phase Cracking Service," Corrosion 10, 149 (1954).

60. O. L. Burns, "Corrosion on a New Distillation Unit Processing Low Sulfur Crude," Corrosion 6, 169 (1950).

61. W. B. Hoyt and R. H. Caughey, "High Temperature Metal Deterioration in Atmospheres Containing Carbon Monoxide and Hydrogen," Corrosion 15, 308t (1959).

62. F. A. Prange, "Corrosion in a Hydrocarbon Conversion System," Corrosion 15, 619t (1959).

63. F. T. Eberle and R. D. Wylie, "Attack on Metals by Synthesis Gas from Methane-Oxygen Combustion," Corrosion 15, 622t (1959).

64. J. R. Schley and F. W. Bennett, "Metallurgical Study of a Unique Failure Mechanism in Gas Cracking Furnace Tubes," Presented at the 21st Annual N.A.C.E. Conference in St. Louis, Missouri, March 15-19, 1965.

65. H. A. Robinson, "Report of the Panel on High Temperature Carburization to the Subcommittee on Corrosion," Minutes of the API's Subcommittee on Corrosion, May 11, 1963.

66. R. F. Hochman, "Metal Deterioration in High Temperature Carbonaceous Environments," Annual Report No. 1, Project No. 2-753, Engineering Experiment Station, Georgia Institute of Technology (1965).

67. R. F. Hochman, "Basic Studies of Metal Deterioration ("Metal Dusting") in Carbonaceous Environments at Elevated Temperatures," Proceedings of the Fourth International Congress on Metallic Corrosion, 258 (1969).

68. H. M. Thron, Jr., "The Effects of Hydrogen, Hydrogen Sulfide and Ammonia on the Elevated Temperature Deterioration of Metals and Alloys in Carbonaceous Gas Environments," M. S. Thesis, Georgia Institute of Technology (1968).

69. R. F. Hochman, "Metal Deterioration in High Temperature Carbonaceous Environments," Annual Report No. 2, Project No. A-753, Engineering Experiment Station, Georgia Institute of Technology (In Print).

70. Gas Carburizing, ASM Committee on Gas Carburizing, American Society for Metals, United States (1964).

71. I. Jenkins, "Gas-Carburizing," Journal of the Iron and Steel Institute (London). 154, 195 (1946).

72. Badische Aniclin and Soda-Fabr., German Patent 293,787 (1913).

73. J. M. Thomas and W. J. Thomas, Introduction to the Principles of Heterogeneous Catalysis, Academic Press, New York (1967).

74. B. T. Brooks, S. S. Kurtz, Jr., C. E. Boord and L. Schmerling, The Chemistry of Petroleum Hydrocarbons 1, Reinhold Publishing Corporation, New York (1954).

75. R. B. Anderson, R. A. Friedal and H. H. Storch, "Fischer-Tropsch Reaction Mechanism Involving Stepwise Growth of Carbon Chains," Journal of Chemical Physics 19, 313 (1951).

76. E. E. G. Hughes and J. M. Thomas, "The Catalyzed Disproportionation of Carbon Monoxide," Fuel 40, 297 (1961).

77. L. A. Haas, S. E. Khalafalla and P. L. Weston, "Kinetics of Formation of Carbon Dioxide and Carbon From Carbon Monoxide in the Presence of Iron Pellets," Bureau of Mines Report 7064 (1968).

78. P. L. Walker, Jr., J. F. Rakszawski and G. R. Imperial, "Carbon Formation Over Iron Catalysts: I. Properties of Iron Formed, and II. Rates of Carbon Formation," Journal of Physical Chemistry 63, 133, 140 (1959).

79. R. V. Westerman, "Mechanism and Kinetics of Iron Deterioration in Carbon Monoxide," Ph.D. Thesis, Georgia Institute of Technology, (1967).

80. T. R. Ratliff, "Early Stages in the Interaction of Carbon Monoxide with Iron Single Crystals," Ph.D. Thesis, Georgia Institute of Technology (1968).

81. W. R. Ruston, M. Warzee, J. Hennant and J. Waty, "The Solid Reaction Products of the Catalytic Decomposition of Carbon Monoxide on Iron at 550°C," Carbon 7, 47 (1969).

82. G. D. Renshaw, C. Roscoe and P. L. Walker, "Disproportionation of CO," Journal of Catalysis 18, 164 (1970).

83. A. R. Cox, "The High Temperature Reaction of Carbon Monoxide with Iron, Nickel, and Austenitic Stainless Steel," M. S. Thesis, Georgia Institute of Technology (1962).

84. W. R. Davis, R. J. Slawson, and G. R. Rigby, "An Unusual Form of Carbon," Nature 171, 756 (1953).

85. L. J. E. Hofer, E. Sterling, and J. T. McCartney, "Structure of the Carbon Deposited from Carbon Monoxide on Iron, Cobalt, and Nickel," Journal of Physical Chemistry 59, 1153 (1955).

86. D. S. MacIver and P. H. Emmett, "Surface-area Measurements on Carbon Black Produced by the Catalytic Decomposition of Carbon Monoxide Over Iron," Journal of Physical Chemistry 59, 1109 (1955).

87. U. Hofmann, "The Deposition of Carbon from Carbon Monoxide and Benzene in the Presence of Iron," Chemische Berichte 61B, 1180 (1928).

88. H. Akamatsu and K. Sato, "Catalytic Decomposition of Carbon Monoxide by Iron," Chemical Society of Japan. Bulletin 22, 127 (1946).

89. S. W. Benson and G. N. Spokes, "Very Low Pressure Pyrolysis," Journal of the American Chemical Society 89, 2325 (1967).

90. S. W. Benson and G. N. Spokes, "Very Low Pressure Pyrolysis," The Journal of Physical Chemistry 72, 1182 (1968).

91. C. A. McDowell, Mass Spectrometry, McGraw-Hill Book Company, New York (1963).

92. Kehl, Principles of Metallographic Laboratory Practice, McGraw Hill Book Company, New York (1949).

93. White, Johnson, and Dantzig, "Chemical Equilibrium in Complex Mixtures," Journal of Chemistry and Physics 28, 751 (1958).

94. Kubert and Stephanov, "Extension of the Rand Method for Determining Equilibrium" Proceedings of the First Conference of the Combustion Institute, Gordon and Breach, New York (1959).

95. "Selected Values of Properties of Hydrocarbons and Related Compounds," American Petroleum Institute Research Project 44, College Station, Texas (1971).

96. P. J. Robinson and K. A. Holbrook, Unimolecular Reactions, Wiley-Interscience, New York (1972).

97. H. Pichler and H. Merkel, U. S. Bureau of Mines Technical Paper 718 (1949).

98. J. F. Shultz, L. J. E. Hofer, K. C. Stein, and R. B. Anderson, "Carbides, Nitrides, and Carbon Nitrides of Iron as Catalysts in the Fischer-Tropsch Synthesis," Bureau of Mines Bulletin 612, 5 (1963).

99. Taylor Lyman, Metals Handbook 1, American Society for Metals, Metals Park, Ohio (1961).

100. S. M. Smith, "Chemical Engineering Kinetics," McGraw-Hill Book Company, New York (1970).

VITA

Michael G. Klett was born in Chicago, Illinois, in April of 1943. He graduated from the Academy of Richmond County, Augusta, Georgia in June of 1961.

He entered the Georgia Institute of Technology in September of 1961. He was awarded the degree of Bachelor of Chemical Engineering in June of 1965.

He entered the Graduate Division of the Georgia Institute of Technology in June of 1965. He was awarded the degree of Master of Science in Chemical Engineering in June of 1967.

He married the former Sylvia Christina Zeagler of Lone Star, South Carolina in June of 1969.